Quaternary Science Reviews 131 (2016) 211–236

Contents lists available at ScienceDirect

Quaternary Science Reviews

journal homepage: www.elsevier.com/locate/quascirev

# Sedimentary architecture and chronostratigraphy of a late Quaternary incised-valley fill: A case study of the late Middle and Late Pleistocene Rhine system in the Netherlands

J. Peeters [a, b, c, *], F.S. Busschers [b], E. Stouthamer [a], J.H.A. Bosch [b], M.W. Van den Berg [b], J. Wallinga [d], A.J. Versendaal [d], F.P.M. Bunnik [e], H. Middelkoop [a]

[a] Utrecht University, Department of Physical Geography, Heidelberglaan 2, P.O. Box 80.115, 3508 TC Utrecht, The Netherlands
[b] TNO – Geological Survey of the Netherlands, Princetonlaan 6, P.O. Box 80.015, 3508 TA Utrecht, The Netherlands
[c] Deltares, Department of Applied Geology and Geophysics, Princetonlaan 6, P.O. Box 85.467, 3508 AL Utrecht, The Netherlands
[d] Soil Geography and Landscape Group, Wageningen University, PO Box 47, 6700 AA Wageningen, The Netherlands
[e] TNO Petroleum Geosciences, Princetonlaan 6, 3584 CB Utrecht, The Netherlands

ARTICLE INFO

*Article history:*
Received 21 February 2015
Received in revised form
30 June 2015
Accepted 1 October 2015
Available online 22 November 2015

*Keywords:*
Eemian interglacial
Incised-valley
Delta
Estuary
Sea level
Preservation
Glacio-isostasy
Palaeogeography
Luminescence dating

ABSTRACT

This paper describes the sedimentary architecture, chronostratigraphy and palaeogeography of the late Middle and Late Pleistocene (Marine Isotope Stage/MIS 6-2) incised Rhine-valley fill in the central Netherlands based on six geological transects, luminescence dating, biostratigraphical data and a 3D geological model. The incised-valley fill consists of a ca. 50 m thick and 10–20 km wide sand-dominated succession and includes a well-developed sequence dating from the Last Interglacial: known as the Eemian in northwest Europe.

The lower part of the valley fill contains coarse-grained fluvio-glacial and fluvial Rhine sediments that were deposited under Late Saalian (MIS 6) cold-climatic periglacial conditions and during the transition into the warm Eemian interglacial (MIS 5e-d). This unit is overlain by fine-grained fresh-water flood-basin deposits, which are transgressed by a fine-grained estuarine unit that formed during marine high-stand. This ca. 10 m thick sequence reflects gradual drowning of the Eemian interglacial fluvial Rhine system and transformation into an estuary due to relative sea-level rise. The chronological data suggests a delay in timing of regional Eemian interglacial transgression and sea-level high-stand of several thousand years, when compared to eustatic sea-level. As a result of this glacio-isostatic controlled delay, formation of the interglacial lower deltaic system took only place for a relative short period of time: progradation was therefore limited. During the cooler Weichselian Early Glacial period (MIS 5d-a) deposition of deltaic sediments continued and extensive westward progradation of the Rhine system occurred.

Major parts of the Eemian and Weichselian Early Glacial deposits were eroded and buried as a result of sea-level lowering and climate cooling during the early Middle Weichselian (MIS 4-3). Near complete sedimentary preservation occurred along the margins of the incised valley allowing the detailed reconstruction presented here.



## 1. Introduction

River deltas and estuaries are world-wide occurring environments where rivers connect to seas and oceans. Their deposits make up an important part of the geological record and are formed in complex sedimentary environments where marine, estuarine and fluvial depositional processes alternate both in space and time. The resulting strong heterogeneous nature of these deposits is critical in determining for example physical characteristics (i.e. net-to-gross ratio, permeability and porosity) in hydrocarbon reservoirs (e.g. Martinius et al., 2005; Thrana et al., 2014), shallow subsurface aquifers (e.g. Bierkens, 1996; Sanchez-Vila et al., 2006), and aggregate resources mining (Van der Meulen et al., 2005). There is a

* Corresponding author. Utrecht University, Department of Physical Geography, Heidelberglaan 2, P.O. Box 80.115, 3508 TC Utrecht, The Netherlands.
*E-mail address:* j.peeters1.uu@gmail.com (J. Peeters).

http://dx.doi.org/10.1016/j.quascirev.2015.10.015
0277-3791/

particular need for high-resolution records, for systems that have been subjected to changes in external forcings, to better understand lower-deltaic sediment records, their preservation over longer timescales and to facilitate their interpretation for various fields of application. Quaternary sequences are suitable candidates for such investigations, as they are still within the practical range of high-density data collection and dating (Blum and Törnqvist, 2000). The Middle and Late Pleistocene southern North Sea Basin record of the Rhine-Meuse system is an example of a record where these prerequisites are met (e.g. Törnqvist et al., 2000, 2003; Wallinga et al., 2004; Busschers et al., 2005, 2007, 2008; Hijma et al., 2012; Peeters et al., 2015).

This record consists of several tens of metres of mostly sandy deposits that were supplied to the basin under cold periglacial conditions (Cohen et al., 2014). Parts of this Rhine-Meuse record contain an embedded sequence of Last Interglacial sediments that were formed under near-coastal conditions (Busschers et al., 2007). Large amounts of digitally available borehole information and series of geological maps (Van der Meulen et al., 2013; TNO-GSN, 2014) and more recently also 3D geological models (Stafleu et al., 2011; Gunnink et al., 2013) now allow study of these sediments at an unprecedented high level of detail. In addition, Rhine sediments have proven to be suitable for luminescence-dating (Wallinga et al., 2004; Busschers et al., 2007) and the well-defined pollen-based regional biostratigraphical framework (Zagwijn, 1961, 1996; Van Leeuwen et al., 2000) enables construction of a high-resolution chronostratigraphical framework. The combination of high data-density and chronological control allows linking of the sedimentary development of the Rhine-Meuse system, and in particular the developments of the Last Interglacial part, to records of climate change, sea-level change and glacio-isostasy.

Deposition of the late Middle and Late Pleistocene Rhine sediments occurred in two local depocentres referred to as the Central Depocentre and the Southern Depocentre (Fig. 1) (Busschers et al., 2007; Peeters et al., 2015). Both the on- and offshore parts of the Southern Depocentre were previously studied in detail (Busschers et al., 2007; Hijma et al., 2012). In this area, however, only basal fragments of the Last Interglacial Meuse sequence have been preserved due to strong truncation by the Meuse itself and later also by the Rhine during the Weichselian, preventing a detailed reconstruction of its sedimentary evolution during the Last Interglacial. In the Central Depocentre, however, a 5–10 m thick unit of Last Interglacial sediments occurs embedded within Late Saalian and Weichselian Pleniglacial age coarse-grained fluvial sands (e.g. Wiggers, 1955; Westerhoff et al., 1987). Here, the Last Interglacial sequence is regarded part of an incised-valley fill (cf. Blum, 1993; Zaitlin et al., 1994; Blum et al., 2013), consisting of several stacked and laterally occurring units of fine-grained fluvial and estuarine flood basin and shallow-marine deposits (Peeters et al., 2015). Previous work primarily focused on the shallow-marine infill of the inherited sub-glacially scoured basins (e.g. Cleveringa et al., 2000; De Gans et al., 2000; Van Leeuwen et al., 2000) and the upstream fluvial dominated part of the sequence in the IJssel basin (e.g. Busschers et al., 2007, 2008). The sedimentary architecture of the lower delta plain of the Rhine -

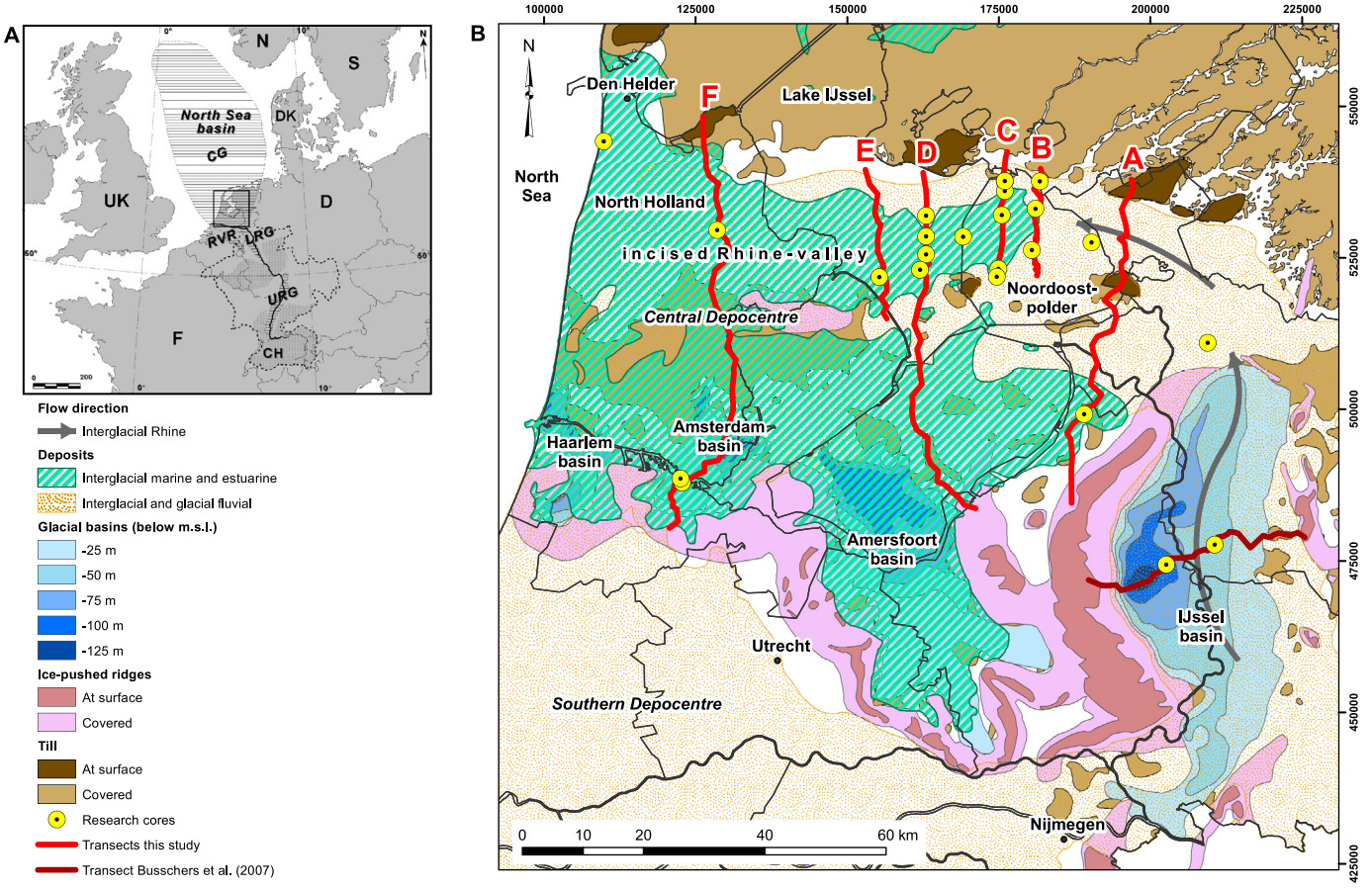


**Fig. 1.** A) The present Rhine drainage basin and its tectonic setting (cf. Ziegler, 1994). Upper Rhine Graben: URG; Lower Rhine Graben: LRG; Roer Valley Graben: RVR; Central Graben: CG. B) Late Pleistocene Rhine and Eemian interglacial marine and estuarine deposits in relation to its inherited Saalian glacio-topography in the central Netherlands. After Peeters et al. (2015), with map data from Gunnink et al. (2013).

including the Last Interglacial estuary - still remains to be studied in detail (Peeters et al., 2015).

In this paper, a high-resolution analysis of the sedimentary architecture and valley-fill succession of the late Middle and Late Pleistocene Rhine-system in the central Netherlands is presented, with emphasis on the Last Interglacial (or 'Eemian interglacial', cf. northwest European chronostratigraphy; Fig. 2) lower Rhine system in the Central Depocentre. This research builds upon thousands of digitally archived borehole descriptions and 5 newly drilled up to 50 m deep continuous sediment cores. For the sediments from these cores, grain-size and sedimentary structures were determined and main depositional units and their bounding surfaces identified. Using these data, six valley-wide geological transects and a series of palaeogeographic maps were constructed. Using 84 newly obtained luminescence-dates and biostratigraphical information (pollen and diatoms) the record was placed in a high-resolution chronostratigraphical framework. The reconstructed changes in sediment characteristics, bounding surfaces, preservation and changes in sedimentary-unit geometry of the Late Pleistocene Rhine system are related to initial conditions and to forcing factors such as climate, sea-level change and glacio-isostatic crustal movements.

## 2. Regional geological setting

The Netherlands and adjacent continental shelf are positioned at the southern margin of the tectonically subsiding Cenozoic North Sea basin (Ziegler, 1994; Van Balen et al., 2005). The overall thickness of the Cenozoic basin fill is ca. 3500 m (Anell et al., 2012). The Quaternary part of this record is up to 900 m thick and consists mainly of fluvial, marine and estuarine sediments (e.g. Zagwijn, 1974, 1989; Caston, 1979). The Central Graben and Roer-Valley-Rift (Fig. 1A) are the main Cenozoic depocentres and form the northern part of the tectonic Rhine Rift System. This system is structurally linked with the Lower and Upper Rhine Graben in Germany (Fig. 1A). These grabens acted as important depocentres, culminating in a Pleistocene Rhine sequence of up to 500 m thick in the central part of the Roer-Valley-Rift (e.g. Zagwijn, 1989; Westerhoff et al., 2008).

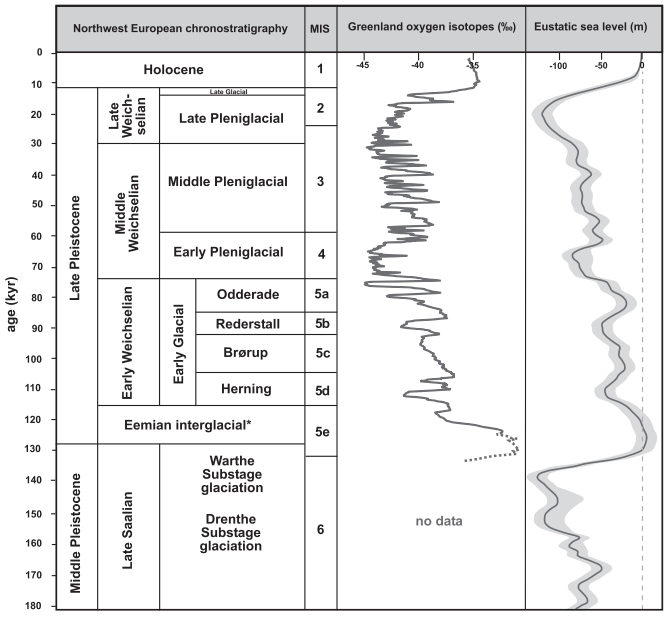


**Fig. 2.** Northwest European chronostratigraphical subdivision of the late Middle and Late Pleistocene (after Peeters et al., 2015 based on Van Huissteden and Kasse, 2001 and Busschers et al., 2007, 2008), with correlations to the marine isotope record (Bassinot et al., 1994) and the Greenland oxygen isotope record (solid-line) from NGRIP-members (2004), supplemented for the Eemian interglacial with data (dashed-line) from NEEM-members (2013). The composite eustatic sea-level curve (dark grey line) and associated confidence interval (light grey area) is from Waelbroeck et al. (2002). *Recently, new insights from Sier et al. (2015) placed the onset of the Eemian in northwestern Europe at ca. 121 ka, thereby post-dating the MIS 6/5e transition by ca. 10 kyr.

Late Pleistocene fluvial deposition was largely controlled by the position of inherited Saalian (Marine Isotope Stage/MIS 6: Fig. 2) glacial morphology, which basically formed two depocentres, separated by a complex of ice-pushed ridges. The Central Depocentre is situated within the area of former ice-cover while the Southern Depocentre is positioned south of it (Fig. 1B). Long-term preservation of Late Pleistocene deposits in both depocentres has been controlled by tectonic subsidence. Subsidence rates range from ca. 0.2 m/ka in the downstream parts, to near zero in the upstream parts (Kooi et al., 1998), which are close to the North Sea basin hinge line.

The study area comprises the Central Depocentre, where in the northern part the Rhine occupied an east-west orientated incised river-valley (incised Rhine-valley: Fig. 1B) during and after melting of the Late Saalian ice-sheet. The sedimentary record of the Central Depocentre partly reflects the infill of this incised-valley and shows a stacked sequence consisting of three main units (each comprising several subunits) with a total thickness of ca. 35 m and a width of ca. 9 km in the upstream (eastern) part, to a total thickness of ca. 55 m and a width of ca. 22 km in the downstream (western) part. The lower Late Saalian to early Eemian units and the upper Weichselian units primarily consist of coarse-grained channel belt deposits. Sandwiched in between is a 5–10 m thick unit that is dominated by fine-grained fluvial and estuarine sediments of Eemian interglacial age (MIS 5e: Fig. 2) (Wiggers, 1955; Peeters et al., 2015). Upstream of the incised valley, the Eemian interglacial fluvial sequence extends into the IJssel basin (Fig. 1B) (Busschers et al., 2007). In the southern part of the Central Depocentre, outside the incised Rhine-valley, Eemian interglacial shallow-marine deposits are found in the sub-glacially scoured basins. These glacial basins reach depths of over 100 m below present-day sea level and are found directly north of a series of pronounced ice-pushed ridges (Fig. 1B).

During and after sea-level fall at the Weichselian Early Glacial to Weichselian Early Pleniglacial transition (Fig. 2), major parts of the Eemian interglacial high-stand prism were eroded by the Rhine. Despite this erosion, significant amounts of Eemian interglacial and Weichselian Early Glacial sediments have been preserved in the Central Depocentre (Busschers et al., 2007; Peeters et al., 2015).

## 3. Material and methods

### 3.1. Data collection

The reconstruction of the late Middle and Late Pleistocene Rhine system was made by means of six valley-wide geological transects established using a framework of ca. twenty-five 25–50 m deep continuous cores, together with thousands of archived borehole descriptions, spectral gamma-ray logs and cone penetration tests (CPTs). The position of the transects was selected after evaluating archived borehole information from the TNO - Geological Survey of the Netherlands (TNO-GSN) subsurface-database (TNO-GSN, 2014) and published data that described the position and geometry of the valley fill (Peeters et al., 2015 and references therein). The transects aimed to penetrate the deepest occurrences of the supposedly Eemian interglacial sequence and to span the full lateral extent of the Late Pleistocene Rhine system (Fig. 1B).

For this study five continuous cores, four spectral gamma-ray borehole logs and twelve CPTs were newly obtained (Fig. 1B), covering all relevant sedimentary units in order to provide additional sedimentary characteristics from these lower-deltaic key-sites and to derive fresh material for analysis and dating. Eighteen cores from published work and archived material were used. An overview of all new and existing research cores and their associated analyses can be found in the Supplementary data (Table S.2).

The new continuous cores were obtained with a truck-mounted Nordmeyer core-sampler, using a steel borehole casing and sediment-catcher, providing undisturbed samples in closed plastic tubes (10 cm diameter and 1 m length). The derived cores were split in halves at the core-description facility of the Geological Survey of the Netherlands. One core-half was used for sedimentary description and reference, whereas the other half was available for luminescence dating and/or biostratigraphic analyses. Detailed lithological and sedimentological core description was performed according to Geological Survey standards (Bosch, 2000).

CPT and spectral gamma-ray measurements were carried out at the same borehole positions in order to verify and determine bounding-surface positions and lithological trends in the cores (cf. Busschers et al., 2007). CPT data was also used to support lithological correlations in between transect boreholes (following the method of Huijzer, 1992 and Coerts, 1996). Three of the new cores and 9 CPTs were collected from open surface water (Lake IJssel: Fig. 1B), using a multi-purpose jack-up barge on which land-based drilling and CPT-equipment was installed.

Information on the subsurface composition in between the six transects was collected by analysing several thousands of archived borehole descriptions from the TNO-GSN subsurface-database (TNO-GSN, 2014) and by using a geological voxel-model (NL3D model) as built and operated by TNO-GSN (Van der Meulen et al., 2013). This model describes the 3D lithological variability of the subsurface in the Netherlands, up to a depth of 50 m below the surface, using voxels (3D cells) of 250 × 250 × 1 m. The input data for this model is the Digital Geological Model (DGM: Gunnink et al., 2013) and about 497.000 borehole descriptions from two subsurface databases: TNO-GSN (2014) and that of Utrecht University (Berendsen et al., 2007). The NL3D model gives a 3D representation of subsurface lithology and can be used to determine the 3D extent of specific sedimentary units identified at transect level.

### 3.2. Sedimentological description and identification of sedimentary units

The sedimentological analysis was carried out conform the methods and concepts of Busschers et al. (2007) for describing sedimentary units of the Rhine system. The analysis comprised the following steps:

1) Facies description at core-level. This involved integration of grain-size data, gravel content, admixtures and sedimentological structures into sedimentary logs. The sedimentary logs were constructed based on new research cores or existing core descriptions, core photos and lacquer peels.
2) Sedimentary units at core-level were identified from the logs, based on intervals of coherent facies-types with corresponding sedimentary characteristics. These units are typically 5–10 m thick, and can be uniform or show a fining-upward or coarsening-upward trend. Nine sedimentary units were identified in the Central Depocentre, and numbered following Busschers et al. (2007, 2008) with additions for the estuarine domain.
3) Sedimentary units were subsequently correlated among the different cores in each transect by laterally tracing bounding surfaces and following sedimentary unit characteristics of archived borehole descriptions, thereby using CPTs and spectral gamma-ray logs from the TNO-GSN subsurface-database (TNO-GSN, 2014).
4) Finally, laterally identified sedimentary units in each transect were correlated in upstream and downstream direction by tracing bounding surfaces through hundreds of archived borehole descriptions (TNO-GSN subsurface database: TNO-GSN, 2014) and by using the NL3D voxel model output.

### 3.3. Chronostratigraphy

Luminescence dating on sand-sized quartz and feldspar grains was used to provide an absolute chronology for the sedimentary units. This method provides a precision of 5% of the age at best (Murray and Olley, 2002; Wallinga, 2002). Palynological analysis on organic and clay bearing material was performed to provide a higher-detailed biostratigraphic framework, enabling to distinguish different periods within the Eemian interglacial (cf. Zagwijn, 1961, 1996). Diatom analysis was performed to reconstruct past local environmental conditions.

#### 3.3.1. Luminescence dating

Both quartz optically stimulated luminescence (OSL) and feldspar post-infrared infrared-stimulated luminescence dating (pIRIR) were performed by the Netherlands Centre for Luminescence dating. Quartz is principally the mineral of choice in optical dating as the OSL signal is most rapidly reset and is stable over geological time (e.g. Wintle, 2008). However, quartz saturates at relatively low doses, which limits the age range of OSL dating (Wintle and Murray, 2006; Murray et al., 2007). Therefore, only OSL dating of quartz grains for the younger (mostly <100 ka) samples was used.

For older samples (mostly >100 ka), feldspar pIRIR dating was used. Feldspar infrared stimulated luminescence (IRSL) signals saturate at higher doses than quartz OSL signals, but conventional IRSL signals are unstable over geological time due to anomalous fading (e.g. Wallinga et al., 2007). As a consequence, feldspar IRSL ages tend to underestimate the burial age of the sediments. Although correction methods have been proposed (e.g. Lamothe et al., 2003; Kars et al., 2008), their application is problematic and may yield inaccurate results (e.g. Wallinga et al., 2007; Kars et al., 2012) and was therefore not applied in this study. Instead, pIRIR signals were used, which have been shown to be less affected by anomalous fading (Thomsen et al., 2008). Reported pIRIR dating tests indicated that pIRIR signals reach saturation levels for infinite age samples and ages in agreement with independent age control (Thiel et al., 2011; Buylaert et al., 2012; Kars et al., 2012). Therefore they were considered applicable to the older (>100 ka) and subaqueous deposited samples (Kars et al., 2014).

For this study 44 new feldspar pIRIR and 40 new quartz OSL samples were obtained from 13 research cores. Samples were taken from relatively homogeneous sand intervals. In addition, 18 luminescence dating results that were reported earlier (i.e. Busschers et al., 2007; Kars et al., 2012) were used (Table S.1). Information on the sediment pre-treatment and data of the dose-rate and equivalent dose measurements (both OSL and pIRIR) is provided in the Supplementary data. For the final age calculations (Table 2) only the measurements with validity-label 'accepted' were used. This validity estimate is based on expert judgement, and takes into account the spread in equivalent dose distributions, likelihood of severe age-overestimation due to poor-bleaching, proximity to luminescence saturation levels, as well as consistency of results compared to overlying and underlying sediment units. Age estimates are reported with a 1 σ uncertainty (68% confidence

interval), which includes random and systematic uncertainties in both equivalent dose and dose rate estimation.

Validity of quartz OSL and feldspar pIRIR ages has convincingly been shown in other studies (e.g. Rittenour, 2008 for quartz OSL; Buylaert et al., 2012 and Kars et al., 2012 for feldspar pIRIR). As a further test for the robustness of the OSL and pIRIR chronologies, quartz OSL and feldspar pIRIR dating results were compared for 33 samples for which both methods were applied in this study. Both methods are not truly independent as they share about two-third of their dose rate, and luminescence signals are measured on the same equipment. However, the equivalent doses are measured on different minerals, and the luminescence signals used have different behaviour regarding bleachability, stability and saturation levels. A comparison of results may therefore provide additional information whether the signals were sufficiently reset prior to deposition and burial (e.g. Murray et al., 2012), whether the signals are sufficiently stable over the period of interest, and whether natural and laboratory dose response curves are identical. Results show that the quartz OSL and feldspar pIRIR results agree reasonably well for all samples where quartz OSL ages were accepted (Fig. 3). For the samples where quartz OSL results were rejected as the mean equivalent dose was too close to saturation (see Supplementary data), dating results were less consistent. For some of these samples, pIRIR yielded substantially older ages which is attributed to underestimation of quartz OSL ages due to artefacts related to OSL signals approaching saturation levels (e.g. Murray et al., 2007). However, even for this dataset the majority of quartz and feldspar results agreed, indicating that the adopted criterion for rejecting the quartz OSL results may be more strict than needed (see e.g. Murray et al., 2002; Wintle and Murray, 2006).

For each of the identified sedimentary units, the median age and 1σ standard deviation was calculated using all accepted OSL and pIRIR dating results following the probability density function method described by Busschers et al. (2007). Here the median age and 1σ standard deviation are taken as best estimate for the timing and duration of deposition of the sedimentary units (Busschers et al., 2007).

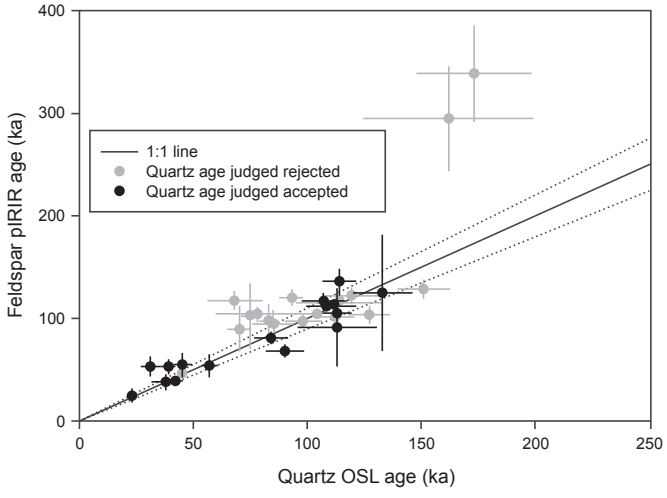


**Fig. 3.** Comparison of quartz OSL and feldspar pIRIR dating results. Samples for which quartz OSL results were judged reliable are shown with black symbols, and samples for which quartz OSL was beyond the applied saturation threshold (see Supplementary data) are indicated with grey symbols. The graph shows an adequate correlation between both luminescence methods, adding to the confidence in the established chronology.

*3.3.2. Palynological and diatom analysis*

In this study, palynological analysis was primarily used as a biostratigraphic correlation tool in order to relate the sedimentary record to the relative Eemian timescale of Zagwijn (1961, 1996). Palynological analysis was done for 7 cores that contained suitable material (Table S.2). The new analysis results were supplemented by pollen records from 10 other locations that were already available in the TNO-GSN subsurface database (Table S.2). Samples were prepared following standard procedures (cf. Faegri and Iversen, 1989). Northwest European regional Pollen Assemblage Zones (PAZ) were determined based on differing taxa assemblages and known Late Pleistocene vegetation-development and responses (cf. Zagwijn, 1961, 1996). Palaeoenvironmental conditions (fresh water, brackish and marine) were reconstructed by diatom analysis for 1 new core (cf. Battarbee, 1973; Cremer et al., 2001) and were available for 5 other locations in the TNO-GSN subsurface database (Table S.2).

## 4. Sedimentary characteristics and chronostratigraphy

In the study area, an incised-valley fill sequence of 9 stacked sedimentary units with a total thickness of ca. 50 m and a maximum width of ca. 25 km was identified. The valley is incised into older deposits - including the Drenthe Substage till (e.g. Fig. 4A–C). Pollen data from the substratum (e.g. core B20F0175: Fig. A.2), shows a typical Holsteinian pollen assemblage including species like *Azolla filiculoides* and *Pterocarya* sp. (Fig. S.4G), indicating a Middle Pleistocene age for the substrate deposits (Florschütz, 1935; Zagwijn, 1973).

The lower part of the incised-valley fill consists of two coarse-grained fluvial sedimentary units (Units S6 and A1), overlain by two fine-grained sedimentary units of fluvial (Unit A2) and estuarine origin (Unit M1). These interglacial deposits are truncated and buried by three coarse-grained fluvial sedimentary units (Units A3, A4 and A5), which are subsequently overlain by local fluvial and aeolian deposits. The upper part of the sequence consists of Holocene sediments. All fluvial sedimentary units were ascribed a Rhine origin on basis of their mineralogical characteristics (i.e. mineral content, colour, gravel and calcium carbonate content; Table 1) and because they can be stratigraphically correlated into the IJssel basin to known Rhine deposits (Busschers et al., 2007, 2008; Peeters et al., 2015).

The sedimentary architecture and stratigraphic position of the sedimentary units is illustrated in the 6 geological transects A–F (Fig. 4A–F; see Fig. 1B for their location). Sedimentary logs and sedimentary unit boundaries, palaeobiological analyses and luminescence dating results of all research cores are shown in Fig. A.1-3 (see Appendix) and Fig. S.6A-B (see Supplementary data). The sedimentary characteristics of each sedimentary unit are described below, and summarised in Table 1, together with their geometry and interpretation.

### 4.1. Unit S6

*4.1.1. Sedimentary characteristics*

Unit S6 primarily consists of poorly sorted, calcium carbonate-rich, coarse-grained (350–2000 μm), greyish-brown coloured sands (e.g. B15G0212-213-214: Fig. A.3), for at least its upper 8–10 m (ca. −35 to −43 m below mean sea level (m.s.l.) in core B15G0211: Fig. S.6B). The sands commonly contain an admixture of Scandinavian granites, Cretaceous limestone and chert gravels of up to a size of 10 cm. These sands are dominated by cross-bedded sedimentary structures and show ca. 2-3 m thick fining-upward sequences of coarse-to medium-grained sands. Occasionally wood fragments are present (e.g. B15G0213: Fig. A.3; B16C0042: Fig. A.1). In the lower portion of this sedimentary unit (ca. −43 to −49.5 m below m.s.l. in core B15G0211: Fig. S.6B), the sediment

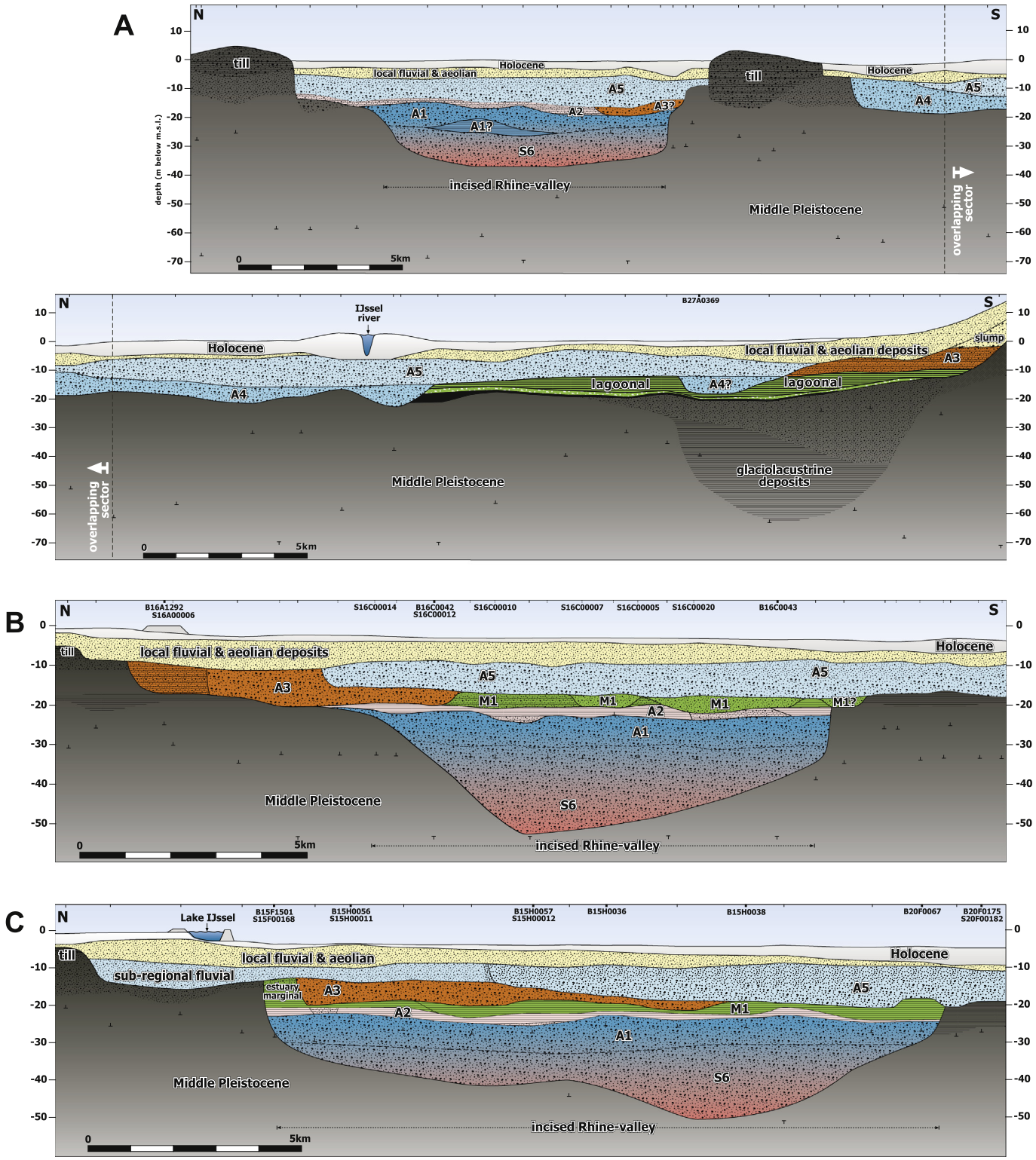


**Fig. 4.** Geological transects showing the sedimentary architecture and stratigraphical position of the sedimentary units from upstream (A) to downstream (F) in the incised Rhine-valley. Transect locations in the Central Depocentre are plotted in Fig. 1B. Please note that transects A, D and F hold southward extensions, positioned *outside* the incised Rhine-valley. The southern section of transect F (Amsterdam glacial basin) is modified after De Gans et al. (2000). Horizontal- and vertical-scales differ between the transects.

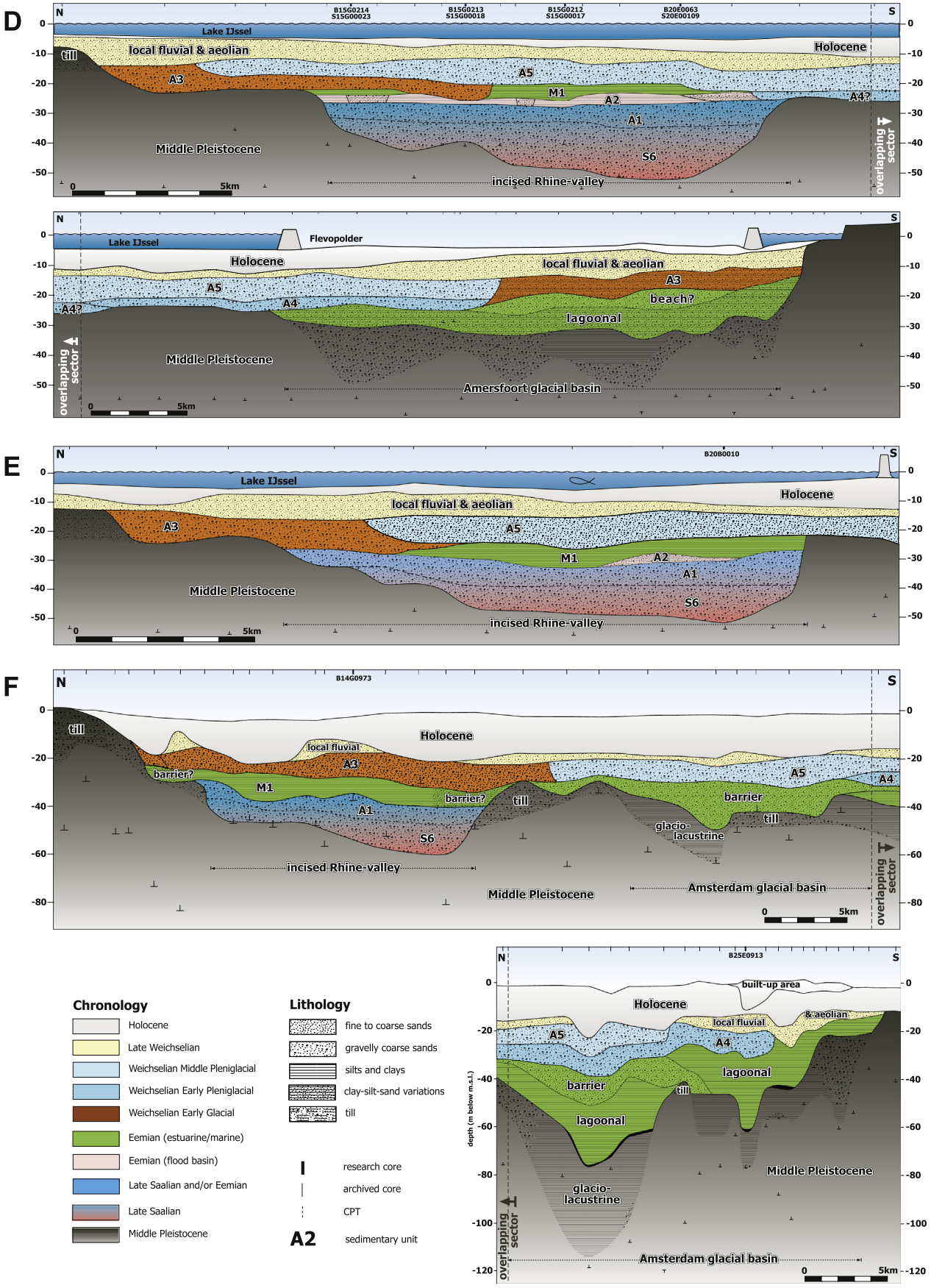


**Fig. 4.** (*continued*).

**Table 1**
Summary of lithology, sedimentary facies, basal bounding surface and geometry of the sedimentary units for geological transects A–F.

| Sedimentary unit | Lithology | Sedimentary facies | Calcium carbonate | Basal bounding surface | Mean thickness (m) | Max thickness (m) | Elevation max (m below m.s.l.) | Elevation min (m below m.s.l.) | Preserved width (km) | Maximum width prior to erosion (km) |
|---|---|---|---|---|---|---|---|---|---|---|
| **Transect A** | | | | | | | | | | |
| A5 | Medium to coarse-grained sands with fine grained top | Amalgamated channel belt | +++ | Erosive | 8 | 10.5 | 4 | 16 | 12 + 23 | 12 + 23 |
| A4 | Medium to coarse-grained sands, gravelly | Channel belt | +++ | Erosive, lag deposit | 5.5 | 10 | 6 | 22.5 | 14 | 14 |
| A3? | Medium to coarse-grained sands, organic-rich with clay-pebbles | Channel belt | +++ | Erosive, lag deposit | 2.5 | 3 | 15 | 19.5 | 2.5 | 12? |
| A3 | Detritus-rich loam/fine sand and peat | Flood basin | ++ | Conformable | 4 | 8 | 3 | 13 | 5 | 28? |
| M1 | *Not present/deposited* | – | – | – | – | – | – | – | – | – |
| A2 | Loam and silts, organic-rich | Fluvial-tidal flood basin | ++ | Conformable, clear lithology change | 2 | 3 | 12 | 19.5 | 9.5 | 11 |
| A1 | Medium to coarse-grained sands | Meandering channel belt | +++ | Conformable, somewhat unclear | 6 | 8.5 | 14.5 | 25.5 | 9.5 | 9.5 |
| S6 | Coarse-grained sands, gravelly | Braided channel belt | +++ | Erosive, gravelly lag deposit | 10.5 | 12 | 23 | 37 | 8.5 | 8.5 |
| **Transect B** | | | | | | | | | | |
| A5 | Medium to coarse-grained sands with fine grained top | Amalgamated channel belt | +++ | Erosive | 8 | 9.5 | 8.5 | 18 | >15 | >15 |
| A4 | *Not present/deposited* | – | – | – | – | – | – | – | – | – |
| A3 | Medium to coarse-grained sands, mollusc(fragments) and clay-pebbles | Channel belt | +++ | Erosive, lag deposit with clay pebbles | 5.5 | 7.5 | 9 | 20 | 7 | 15? |
| M1 | Silty clays, mollusc-rich, and fine-grained sands | Bayhead delta | +++ | Conformable | 3 | 3.5 | 17 | 21 | 9 | ≥11 |
| A2 | Loam, silts, fine sands, organic-rich | Fluvial-tidal flood basin | ++ | Conformable, clear lithology change | 2.5 | 4 | 20 | 24.5 | 11 | 11 |
| A1 | Medium to coarse-grained sands | Meandering channel belt | +++ | Conformable, somewhat unclear | 7 | 7.5 | 22.5 | 31 | 10 | 10 |
| S6 | Coarse-grained sands, gravelly | Braided channel belt | +++ | Erosive, gravelly lag deposit | 12 | 22 | 29 | 52.5 | 9 | 9 |
| **Transect C** | | | | | | | | | | |
| A5 | Medium to coarse-grained sands with fine grained top | Amalgamated channel belt | +++ | Erosive | 8.5 | 11 | 9 | 20.5 | >12 | >12 |
| A4 | *Not present/deposited* | – | – | – | – | – | – | – | – | – |
| A3 | Medium to coarse-grained sands, mollusc(fragments) and clay-pebbles | Channel belt | +++ | Erosive, lag deposit with clay pebbles | 4.5 | 7 | 13 | 20 | 10 | 11? |
| M1 | Silty clay, mollusc-rich | Central-estuary basin + estuary marginal | +++ | Conformable | 3 | 7.5 | 13 | 24 | 15.5 | 15.5 |
| A2 | Loam and silts, organic-rich | Fluvial-tidal flood basin | ++ | Conformable, clear lithology change | 2 | 3.5 | 20.5 | 25.5 | 15.5 | 15.5 |
| A1 | Medium to coarse-grained sands | Meandering channel belt | +++ | Conformable, somewhat unclear | 7.5 | 8.5 | 23 | 33 | 15.5 | 15.5 |
| S6 | Coarse-grained sands, gravelly | Braided channel belt | +++ | Erosive, gravelly lag deposit | 12.5 | 20 | 30.5 | 52 | 14.5 | 14.5 |
| **Transect D** | | | | | | | | | | |
| A5 | Medium to coarse-grained sands | Amalgamated channel belt | +++ | Erosive | 7.5 | 10 | 12 | 22.5 | 43 | 43 |
| A4 | Medium to coarse-grained sands, gravelly and mollusc(fragments) | Channel belt | +++ | Erosive, lag deposit | 3 | 4 | 20 | 26 | 25 | 25 |
| A3 | Medium to coarse-grained sands, mollusc(fragments) and clay-pebbles | Channel belt | +++ | Erosive, lag deposit with clay pebbles | 5.5 | 9 | 14 | 26 | 12 | 12? |
| A3 | Detritus-rich loam/fine sand and peat | Flood basin | ++ | Conformable | 6.5 | 9 | 10 | 21 | 5.5 | 54? |
| M1 | Silty clay, mollusc-rich | Central-estuary basin | +++ | Conformable | 3 | 5.5 | 20 | 26 | 2 + 8 | ≥16 |

**Table 1** (*continued*)

| Sedimentary unit | Lithology | Sedimentary facies | Calcium carbonate | Basal bounding surface | Mean thickness (m) | Max thickness (m) | Elevation max (m below m.s.l.) | Elevation min (m below m.s.l.) | Preserved width (km) | Maximum width prior to erosion (km) |
|---|---|---|---|---|---|---|---|---|---|---|
| A2 | Loam and silts, organic-rich | Fluvial-tidal flood basin | ++ | Conformable, clear lithology change | 2.5 | 3 | 23 | 28 | 14 | ≥15 |
| A1 | Medium to coarse-grained sands | Meandering channel belt | +++ | Conformable, somewhat unclear | 7 | 9 | 25.5 | 35 | 14 | 14 |
| S6 | Coarse-grained sands, gravelly | Braided channel belt | +++ | Erosive, gravelly lag deposit | 12 | 17 | 32 | 51.5 | 13.5 | 13.5 |
| **Transect E** | | | | | | | | | | |
| A5 | Medium to coarse-grained sands | Amalgamated channel belt | +++ | Erosive | 7.5 | 10 | 13.5 | 26.5 | >15 | >15 |
| A4 | Not present/deposited | – | – | – | – | – | – | – | – | – |
| A3 | Medium to coarse-grained sands, mollusc(fragments) and clay-pebbles | Channel belt | +++ | Erosive, lag deposit with clay pebbles | 6.5 | 9 | 13 | 28 | 10 | 10? |
| M1 | Silty clay, mollusc-rich | Central-estuary basin | +++ | Conformable | 5.5 | 6.5 | 21.5 | 33 | 11.5 | 15 |
| A2 | Loam and silt, organic-rich | Fluvial-tidal flood basin | ++ | Conformable, clear lithology change | 2.5 | 4 | 28 | 32 | 3.5 | ≥3.5? |
| A1 | Medium to coarse-grained sands | Meandering channel belt | +++ | Conformable, somewhat unclear | 7 | 9 | 26.5 | 39 | 14.5 | 14.5 |
| S6 | Coarse-grained sands, gravelly | Braided channel belt | +++ | Erosive, gravelly lag deposit | 8 | 12.5 | 32 | 52 | 12.5 | 12.5 |
| **Transect F** | | | | | | | | | | |
| A5 | Medium to coarse-grained sands | Amalgamated channel belt | +++ | Erosive | 8.5 | 12 | 16 | 39 | 40 | 40 |
| A4 | Medium to coarse-grained sands, gravelly and mollusc(fragments) | Channel belt | +++ | Erosive, lag deposit | 8 | 10 | 16.5 | 38.5 | 17 | 17 |
| A3 | Medium to coarse-grained sands, mollusc(fragments) and clay-pebbles | Channel belt | +++ | Erosive, lag deposit with clay pebbles | 8 | 11 | 16 | 34 | 23 | ≥23? |
| M1 | Medium-grained sands, silty clay, mollusc-rich | Estuary-mouth sand-body | +++ | Conformable | 7.5 | 12 | 23 | 40 | 22 | 22 |
| A2 | *Not present/deposited* | – | – | – | – | – | – | – | – | – |
| A1 | Medium to coarse-grained sands | Meandering channel belt | +++ | Conformable, somewhat unclear | 5 | 8 | 28.5 | 48 | 17 | 17 |
| S6 | Coarse-grained sands, gravelly | Braided channel belt | +++ | Erosive, gravelly lag deposit | 7.5 | 12 | 34 | 60 | 16 | 16 |

is more whitish-coloured and appeared to be dissected by the brownish-coloured upper part. In the continuous cores a channel lag deposit is present (ca. 43 m below m.s.l. in core B15G0211: Fig. S.6B). However, since this boundary could not be identified in lower-quality cores, the sediments were lumped into one unit.

The base of Unit S6 is characterised by a marked erosional surface, covered by a gravel lag consisting of coarse-grained sands and gravels (e.g. B15G0212-0214 in Fig. A.3; Fig. S.5E; Fig. S.5H). Its lithology clearly contrasts with the underlying Middle Pleistocene sediments of which the top is generally characterised by pale-coloured, fine-grained (<200 μm) sands that are often rich in detritus and mica flakes (e.g. Fig. A.3).

#### 4.1.2. Geometry

The width of Unit S6 increases in downstream direction from ca. 8.5 km in transect A (Fig. 4A) to 20 km in transect F (Fig. 4F). Its thickness varies on average between 10 and 12 m with maxima up to 20 m (Table 1). The cross-sectional shape of the sedimentary unit is asymmetrical with its maximum depth located in the southern half of the incised valley (e.g. Fig. 4F). The erosive base of Unit S6 represents the basal bounding surface of the incised valley, and rapidly drops by ca. 15 m from its upstream (ca. 35 m below m.s.l. in transect A: Fig. 4A) to its more central part (ca. 50 m below m.s.l. in transect B: Fig. 4B).

#### 4.1.3. Interpretation

The coarse-grained, poorly sorted sediments of Unit S6 are interpreted as fluvial channel belt deposits and reflect a stack of superimposed bar and dune bed forms. The few metre thick sequences indicate that the channel belt was braided (cf. Miall, 1996; Bridge, 2003). The noticeable change from whitish to brownish-coloured sands most likely illustrates a decrease in fluvio-glacial contribution from eastern sources and an increase of Rhine influence from the south (see section 5 below). The latter sediments correspond with the brownish Rhine deposits as found in the IJssel basin (Busschers et al., 2008: their Unit S6).

#### 4.1.4. Chronology

Luminescence dating provided a 1σ age range of 119–143 ka (median age: 130 ka; Table 2) for the Unit S6 sediments. Combined with the stratigraphic position of the sedimentary unit, this indicates that deposition occurred *after* the Drenthe Substage

**Table 2**
Luminescence probability density function-ages per sedimentary unit.

| Sedimentary units | Number of dates | Age (ka) M50 | Age (ka) M16 | Age (ka) M84 |
|---|---|---|---|---|
| Unit A5 | 13 | 43 | 37 | 54 |
| Unit A4 | 5 | 57 | 47 | 69 |
| Unit A3 | 17 | 101 | 78 | 126 |
| Unit M1 | 2 | 110 | 102 | 119 |
| Unit A2 | 4 | 113 | 104 | 122 |
| Unit A1 | 9 | 116 | 106 | 133 |
| Unit S6 | 3 | 130 | 119 | 143 |
| Shallow-marine | 6 | 105 | 88 | 118 |
| Local fluvial and aeolian | 10 | 22 | 14 | 33 |
| Glaciolacustrine | 3 | 121 | 111 | 137 |

A complete overview of all individual luminescence dating results can be found in Table S.1 in the Supplementary data.

deglaciation but still *during* the Late Saalian (MIS 6), i.e. during the Warthe Substage glaciation (Fig. 2).

### 4.2. Unit A1

#### 4.2.1. Sedimentary characteristics

Unit A1 consists of moderately sorted, medium- to coarse-grained (180–600 μm), grey-brown coloured, calcium carbonate-rich sands (e.g. B15G0212-213-214: Fig. A.3). The top of the sedimentary unit is sporadically rooted and grades upward into finer sands (e.g. B15G0213; B15G0214: Fig. A.3). Unit A1 shows cross-bedded structures (2–3 m thick) with varying admixtures of detritus, mica flakes and gravel (e.g. B15G0212-214: Fig. A.3) and locally fining-upward sequences of 3–5 m thickness.

The boundary with underlying Unit S6 is at some locations difficult to determine due to the absence of a clear channel lag deposit. Nevertheless, Unit A1 generally has a more greyish appearance due to a higher clay content, contains more admixtures (clay pebbles, organic debris) and in many cores shows clear cross-bedded structures (e.g. B15G0212-214: Fig. S.5D; Fig. S.5H).

#### 4.2.2. Geometry

Unit A1 spans the entire width of the incised valley and is on average 6.5 m thick (Table 1). The width of Unit A1 increases from 9.5 km at the upstream position of transect A (Fig. 4A) to 21 km at the downstream position of transect F (Fig. 4F).

#### 4.2.3. Interpretation

The moderately sorted coarse- and medium-grained, cross-bedded sands are interpreted to represent fluvial channel belt sands of Rhine origin. The fining-upward sequences (e.g. B15G0212-213-214: Fig. A.3) suggest deposition by channel belts of a meandering fluvial-style (cf. Miall, 1996; Bridge, 2003).

#### 4.2.4. Chronology

Towards the base of Unit A1 a herb, heathland and boreal forest pollen assemblage, characteristic for regional pollen zone LS (cf. Zagwijn, 1961) of the latest Saalian period (PAZ LS: Fig. A.2; Fig. 5) is

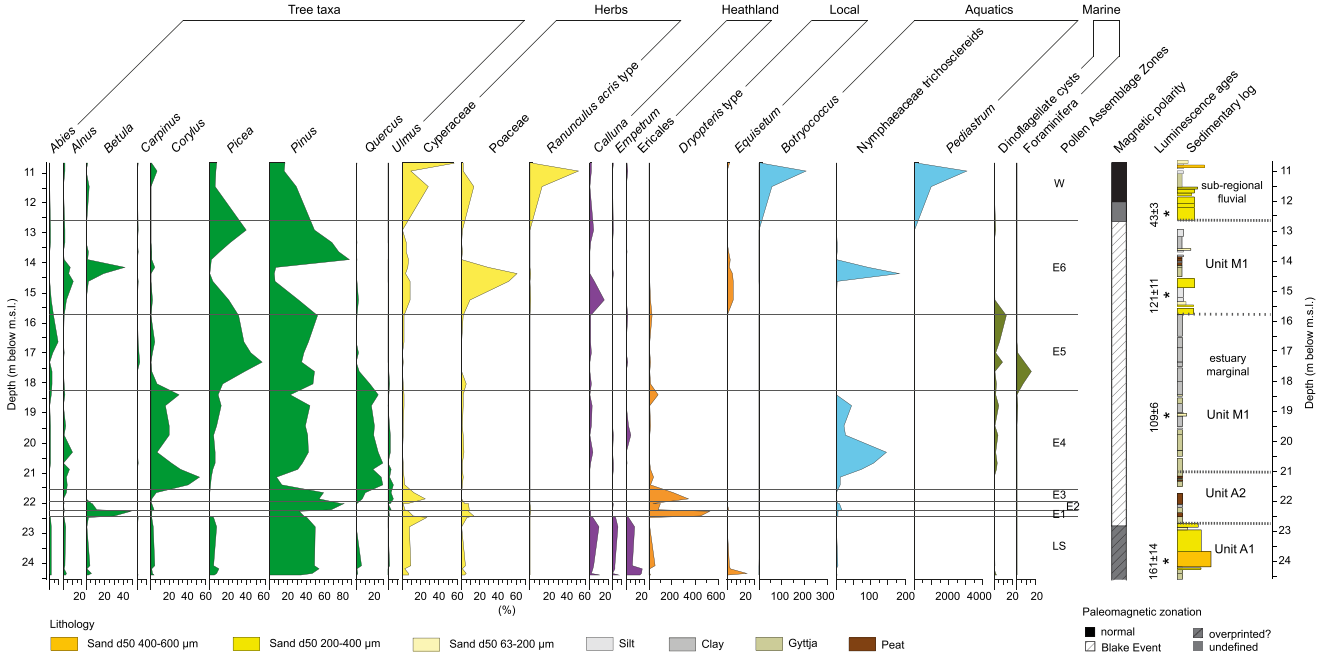


**Fig. 5.** Simplified pollen percentage diagram of research core B15F1501 with regional Pollen Assemblage Zones cf. Zagwijn (1961, 1996). Pollen percentages were calculated based on a pollen sum of trees, upland herbs and heaths. The pollen-sum ranges between 32 and 306 pollen grains, but well exceeded 100 in most (n = 33) samples. Marine indicators identified in the palynological assemblages are also presented. The paleomagnetic polarity is adopted from Sier et al. (2015). Details concerning the palaeomagnetic investigation and identification of the Blake Event in core B15F1501 – their 'Rutten core' – can be found in Sier et al. (2015). See the Supplementary data for all new pollen percentage diagrams used in this study.

found. The upper part of Unit A1 is characterised by a pronounced occurrence of *Betula* and *Pinus* which is indicative for regional pollen zones E1 and E2 (PAZ E1/E2 in B15G0212: Fig. A.3; Fig. S.4B and B15G0214: Fig. A.3; Fig. S.4D), representing the onset of the Eemian interglacial (Zagwijn, 1961, 1996). Luminescence dating of Unit A1 samples give a 1σ age range of 106–133 ka (median age: 116 ka; Table 2), indicating an age falling within the Eemian interglacial and Weichselian Early Glacial (MIS 5: Fig. 2).

### 4.3. Unit A2

#### 4.3.1. Sedimentary characteristics

The base of Unit A2 consists of alternating peat and clay-rich gyttja layers (e.g. B15F1501; S15F00168 and B15G0213 (Fig. 4C; Fig. A.2; Fig. S.5B and S16C00012/00014 (Fig. A.1)) that grade upwards into alternations of laminated loams and silts (e.g. B15G0212 Fig. S.5G). These sediments often contain plant-remains, mica flakes and/or fresh-water molluscs (e.g. *Bithynia* sp.) (e.g. cores B15H0056 and B15H0038: Fig. A.2; cores B15G0212-0213-0214: Fig. A.3; cores B16C0042-0043: Fig. A.1). Fine-to medium-grained, loamy sands with a thickness of ca. 1–2 m sporadically occur in Unit A2 (e.g. S16C00010 and S16C00020: Fig. A.1; B15H0057 and S15H00012: Fig. A.2; B15G0214 and S15G00023: Fig. A.3).

Pollen records originating from the central part of the incised valley (Fig. 5; Fig. S.4A–D), show the presence of *Alnus* and aquatic (fresh water) species (e.g. *Nymphaeaceae*, *Typha latifolia*) from the base of Unit A2 upward. A relative immature paleosol occasionally occurs at the top of the Unit A2 deposits (e.g. research core B15G0213-214: Fig. A.3).

#### 4.3.2. Geometry

Unit A2 has a fairly constant thickness of ca. 2.5 m throughout its entire extent (Table 1), reaching from far upstream in the IJssel basin (Busschers et al., 2007; their transect Fig. 4, see Fig. 1B for its location), via core B21G0547 (Fig. S.6B), up to the central part of the incised valley at the location of transect E (B20B0010: Fig. 4E; Fig. S.6A). Further downstream this sedimentary unit is absent. Its width increases in downstream direction from 9.5 km (transect A: Fig. 4A) to ca. 15 km (transect D Fig. 4D). Unit A2 conformably overlies Unit A1 (e.g. B15G0214: Fig. S.5G) and is clearly distinguished because of its different lithological composition.

#### 4.3.3. Interpretation

The peat and clay-rich gyttja at the base of Unit A2 reflect tranquil conditions of a fluvial wetland environment, which in its turn represents the onset of a drowning sequence which continues upward into the more clastic dominated (silt and clay) part of Unit A2. On basis of the distinct layering of the deposits in combination with the palaeoecological indications, Unit A2 is interpreted as a fluvial-tidal flood basin deposit. This sedimentary unit shows resemblance with the Early Holocene Terbregge Member (Hijma et al., 2009). The occasional immature paleosol at the top of the flood basin deposits reflects periods of decreased fluvio-hydraulic conditions and/or silting-up presumably due to the switching of river branches. The sporadically occurring fine-to medium-grained loamy sands of 1–2 m thick, which are surrounded by finer-grained flood basin sediments, are interpreted as multi-channel deposits of an anabranching fluvial-system (cf. Nanson and Knighton, 1996), on basis of their small dimensions and local occurrence.

#### 4.3.4. Chronology

Pollen analysis shows a dominance of three superimposed vegetation zones that reflect the succession of a (warm) temperate forest (e.g. cores B15F1501: Fig. 5, Fig. S.4A; B15G0212-0213-0214: Fig. S.4B–C-D; B20E0063: Table S.2). The lower zone is characterised by *Pinus*, *Ulmus* and *Quercus* which is indicative for Eemian PAZ E2 (Zagwijn, 1961, 1996). The central zone is dominated by *Quercus* and *Corylus* and shows strong resemblance with Eemian PAZ E3 (Zagwijn, 1961, 1996). The assemblage in the uppermost zone, with a strong dominance of *Corylus*, is typical for Eemian PAZ E4a (Zagwijn, 1961, 1996). Upstream of the fluvial-tidal flood basin, the top of Unit A2 deposits contain pollen assemblages which are dominated by *Carpinus*, *Picea* and *Pinus* pollen (e.g. core B21G0547: Table S.2; core B27H0282: Busschers et al., 2007), representing Eemian interglacial pollen zones E5 and E6 respectively (Zagwijn, 1961, 1996). This implies diachroneity with the downstream portion of the Eemian interglacial flood basin deposits. Luminescence dating of Unit A2 sediments gives a 1σ age range of 104–122 ka (median age: 113 ka; Table 2) suggesting an Eemian interglacial and Weichselian Early Glacial age (MIS 5: Fig. 2).

### 4.4. Unit M1

#### 4.4.1. Sedimentary characteristics

Unit M1 is characterised by green-grey coloured, glauconite-bearing silty clays that are often horizontally laminated. The clays contain detritus and micas (e.g. core B15F1501: Fig. A.2; Fig. S.5A-B and cores B15G0212/0214: Fig. A.3; Fig. S.5D/G) and predominantly occur along the central axis of the incised valley. The clays frequently contain abundant marine molluscs (e.g. *Bittium reticulatum*, *Venerupis senescens*; e.g. B15H0036, B15H0038 and B20F0067: Fig. A.2). Along the northern margin of the incised valley (e.g. cores B15F1501 and B15H0056: Fig. A.2) brackish and marine mollusc species are absent and only thin-walled fresh-water mollusc-fragments occur. Besides the characteristic clay, medium-grained (150–330 μm) silty sands occur within Unit M1 at the most downstream portion of the incised valley (i.e. transect F) along its northern and southern margins (Fig. 4F). These deposits commonly contain marine mollusc fragments and occasionally wood debris and gravel at its base. Upstream in the central part of the valley (i.e. transect B: Fig. 4B), CPT results indicate that silty clays locally alternate laterally with fine-grained sands (e.g. S16C00005/00007/00010: Fig. A.1).

The palaeoecological record of Unit M1 (core B15F1501: Fig. A.2) shows a transition from a fresh water and fresh/brackish water diatom assemblage (ca. −21 to −19 m below m.s.l.) via a more mixed fresh/brackish/marine diatom assemblage (ca. −19 to −17.5 m below m.s.l.) towards a marine dominated assemblage (ca. −17.5 to −16 m below m.s.l.) with abundant diatoms of *Martyana martyi* and *Opephora* sp. (Fig. 6) and other marine indicators like *Dinoflagellates* and *Foraminifers* (Fig. 5). Towards the top of Unit M1 at −13 m below m.s.l. fresh water and fresh/brackish water diatom species like *Staurosirella* sp. and *Cocconeis* sp. dominate while marine indicators disappear.

South of the Eemian interglacial Rhine estuary, in the southern part of the Central Depocentre (Fig. 1), a shallow-marine embayment was located during the Eemian interglacial (e.g. Cleveringa et al., 2000; De Gans et al., 2000; Van Leeuwen et al., 2000). Here, medium-grained barrier and beach sands with occasional mollusc concentrations and silty, low-energetic lagoonal clays were deposited in the former glacial basins of Amsterdam (Fig. 4F) and Amersfoort (e.g. core B27A0369: Fig. 4A; Fig. S.6A). These basins, which were topographically separated from the interior shelf sea and outer-estuary by sills at depths of 35–40 m below m.s.l. (Cleveringa et al., 2000; De Gans et al., 2000), contain a near-complete Eemian interglacial record that was extensively studied in the past (Amersfoort basin: Zagwijn, 1961, 1983; Cleveringa

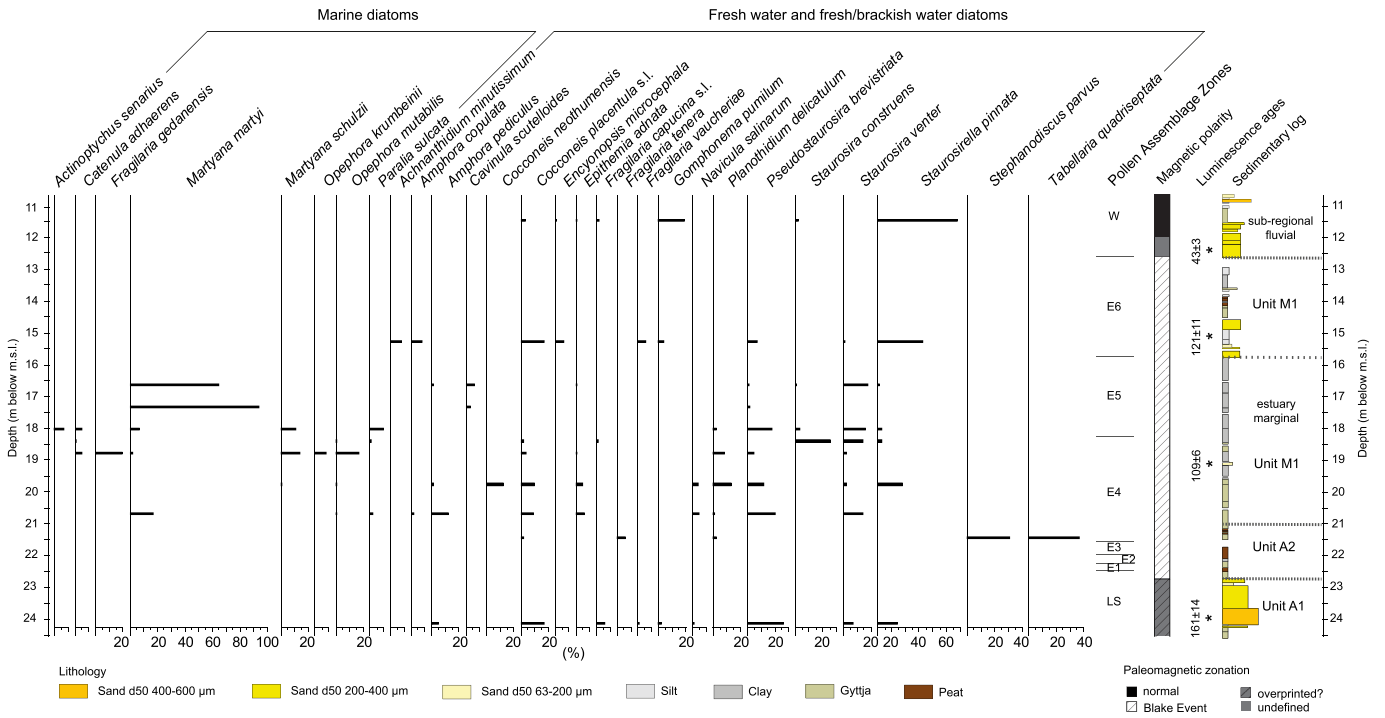


**Fig. 6.** Percentage diagram of diatom analysis of research core B15F1501. The diatom taxa are divided in a marine diatoms-group and a fresh water and fresh-brackish water diatoms-group. The paleomagnetic polarity is adopted from Sier et al. (2015).

et al., 2000; Amsterdam basin: Zagwijn, 1983; De Gans et al., 1987, 2000; Van Leeuwen et al., 2000; Beets and Beets, 2003; Beets et al., 2006).

### 4.4.2. Geometry

Unit M1 is found as far upstream as the central part of the Noordoostpolder (i.e. transect B: Fig. 4B), where it has an average thickness of 3 m and a width of 9 km. The width of this sedimentary unit considerably increases in downstream direction (i.e. transect F) to a maximum of 22 km (Fig. 4F), spanning the entire width of the incised valley. The thickness of the sedimentary unit increases in downstream direction too, from 3 m (Fig. 4B) up to 7.5 m (Fig. 4F; Table 2). Unit M1 conformably overlies Unit A2 (e.g. B15F1501: Fig. S.5B; B15G0212/214: Fig. S.5D/G) from which it can primarily be distinguished on basis of its differing lithology (clay vs. loam) and the occurrence of marine molluscs.

The medium-grained silty sands of Unit M1 are only present at the most downstream portion of the incised valley at the position of transect F (Fig. 4F). Here the deposits have a thickness of ca. 4–6 m and a width of ca. 2–4 km. The deposits appear to onlap onto the sides of the incised valley (Fig. 4F).

The laterally alternating silty clays and fine-grained sands as deduced from the CPT results, only occur at the most upstream limit of the estuary at the position of transect B (Fig. 4B), where they reach a thickness of ca. 3–4 m. Their lateral extent differs over the transect, but suggests a minimum width of ca. 1 km and a maximum width of up to 3 km.

### 4.4.3. Interpretation

The fine-grained nature and colour of the sediments, together with their palaeoecological content, sedimentological characteristics and the regional geological context suggests deposition in an estuarine environment (cf. Dalrymple et al., 1992; Dalrymple and Choi, 2007) and represent the ongoing drowning of the fresh-water fluvial-tidal flood basin (Unit A2). This drowning is demonstrated in the palaeoecological record of core B15F1501 (Fig. 6), showing a transition from fresh via brackish water towards marine conditions. This illustrates the ongoing Eemian transgression of the incised Rhine-valley by marine waters, culminating in a high-stand during PAZ E5 (Fig. 5), followed by regression.

The longitudinal and lateral changes as observed in Unit M1, resemble the estuarine tripartition of Dalrymple et al. (1992) into 1) an upper-estuary bay-head delta area where the river enters the central basin, 2) a fine-grained, muddy central estuary basin and 3) an estuary-mouth sand-body: comprising barrier, wash-over, tidal inlet and tidal delta deposits in the outer-estuary.

The geometry, stratigraphic and spatial position of the fine-grained sands as observed in the most upstream extent of the Rhine estuary (i.e. transect B: Fig. 4B), suggest deposition in a bay-head delta-complex. The sands seem to connect to fine- to medium-grained upstream channel belts in the IJssel basin, which presumably formed the source for the bay-head delta sediments.

The laminated silty clays that are common in Unit M1 (Figs. 4C–E) are interpreted to reflect the lack in supply of sand towards the central and downstream parts of the estuary due to upstream sediment trapping and storage in the bay-head delta complex. This feature is in analogy with the situation during transgression in the Early Holocene Rhine-Meuse delta in the western Netherlands (Hijma et al., 2009). These fine-grained deposits are interpreted as the central-estuary basin.

The silty medium-grained sands with marine molluscs that are found in isolated positions at the margins of the incised valley in the far downstream part of the estuary are more difficult to interpret. Within the context of the upstream–downstream transitions described above they are however thought to represent (parts of) the estuary-mouth sand body (cf. Allen, 1991; Allen and Posamentier, 1993). These sediments occasionally contain reworked gravel at

their base, which originates from the underlying fluvial and glacial deposits present at this location (Fig. 4F).

#### 4.4.4. Chronology

The pollen record in Unit M1 shows a dominance of (warm) temperate tree-pollen. At some downstream sites (e.g. research cores B14G0973: Fig. S.6A; B15G0212/214: Fig. A.3) the base of Unit M1 is characterised by PAZs E2, E3 and E4a (Fig. S.4B and S.4D). The main part of the pollen record of Unit M1 (e.g. research cores B15F1501: Fig. 5; Fig. S.4A and B15G0212/214: Fig. S.4B and S.4D), is however characterised by *Taxus* and *Carpinus* pollen (PAZ E4b and E5 respectively: cf. Zagwijn, 1961), reflecting the Eemian interglacial vegetation optimum (Zagwijn, 1996). In core B15F1501 *Carpinus* percentages in PAZ E5 are relatively low, when compared to the diagrams of Amersfoort (Zagwijn, 1961) and Amsterdam-Terminal (Van Leeuwen et al., 2000). This difference is explained as a regional effect: the high values encountered in the southern part of the Central Depocentre are due to the vicinity of the ice-pushed ridges with dryland forests. In the vicinity of core B15F1501, located in the northern part of the Central Depocentre, less dryland forest area was present to accommodate *Carpinus* expansion. At the top of Unit M1 in core B15F1501 (Fig. 5; Fig. S.4A), also the *Picea* and *Pinus* dominated PAZ E6 is found. Luminescence dating of samples (n=2) from Unit M1 give a 1σ age range of 102–119 ka (median age: 110 ka; Table 2), suggesting a late Eemian interglacial and Weichselian Early Glacial age (MIS 5: Fig. 2).

In addition to the earlier work on the shallow-marine embayment in the southern part of the Central Depocentre (e.g. Cleveringa et al., 2000; De Gans et al., 2000; Van Leeuwen et al., 2000), a series of luminescence dates has now become available from these deposits. Luminescence datings of these sediments – inseparably forming part of the marine transgression - provided a 1σ age range of 88–118 ka (median age: 105 ka; Table 2), indicating a late Eemian interglacial and Weichselian Early Glacial age (MIS 5: Fig. 2) which is largely in agreement with the dating results presented for the Rhine estuary.

### 4.5. Unit A3

#### 4.5.1. Sedimentary characteristics

In the western part of the study area most of Unit A3 consists of grey-brown, calcium carbonate-rich, coarse- to medium-grained sands (650-200 μm) (Fig. 4B–F). Here, the lower 1–3 m of Unit A3 generally shows a coarsening-upward trend and an increase in the amount of gravel (Fig. A.1-3). Internally, sand grain-size can however vary over short vertical distances. In this area the sedimentary unit is also characterised by abundant clay pebbles, peat fragments, marine-mollusc fragments and organic debris (e.g. B15G0213-214: Fig. A.3; Fig. S.5G). The coarser-grained lower part of the sedimentary unit is generally overlain by relative finer-grained sands and silts with no clear grain-size trends. Especially in cases where the upper part of Unit A3 consists of silt, this transition is very sharp. In the southeastern part of the Central Depocentre (south of the incised valley; Fig. 4A–D), Unit A3 is generally finer-grained and is characterised by alternating decimetre thick humic clay, peat and sand layers (cf. Busschers et al., 2007).

In the western part of the incised Rhine-valley the grain-size of Unit A3 decreases, the amount of clay increases and fining upward sequences start to dominate (Fig. 4F). This especially applies to the most northwestern part of Unit A3 (transect F) where the sediments are characterised by an alternation of brownish and greyish detritus-rich silty clay and 1–3 m thick fine-grained sands (e.g. B14A0090: Fig. S.6B). Here the sedimentary unit is capped by a 1–2 m thick wood-rich peat. The fine-grained sands are typically admixed with mica flakes, a component that together with their slightly higher clay content makes them distinguishable from overlying sediments of local origin (described below in section 4.8).

A temporary construction site that was situated east of Den Helder in 1976 (Fig. 1B; RGD, 1977) exposed the top level of Unit A3 at ca. 15 m below m.s.l. The Unit A3 sediments here, were described as fine-grained cross-laminated Rhine sands deposited in an unidirectional westward directed flow.

#### 4.5.2. Geometry

Unit A3 is present along the entire northern margin of the incised valley, except for the most upstream transect A (Fig. 4A) where these deposits are presumed to have been eroded by younger Rhine channels. The maximum width of Unit A3, prior to erosion, is estimated to have been ca. 54 km at the position of transect D (Fig. 4D).

The base of this sedimentary unit has a strong erosive character and deeply truncates Unit M1 (e.g. B15G0213 and S15G00018: Fig. 4D; Fig. A.3 and B16C0042 and S16C00014: Fig. 4B; Fig. A.1) and older Middle Pleistocene sediments (e.g. B16A1292 and S16A00006: Fig. 4B; Fig. A.1 and Fig. 4D–E). Locations where erosion by younger Rhine channels was absent show that the sedimentary unit increases in thickness from ca. 6 m at the location of transect B to ca. 11 m at the location of transect F. In its most northwestern occurrence, Unit A3 reaches a thickness of ca. 15 m (e.g. B14A0090: Fig. S.6B), showing that the thickness increases in westward direction.

#### 4.5.3. Interpretation

The brownish coloured carbonate-rich sands of Unit A3 are interpreted as fluvial channel belt sediments of Rhine origin. The silts and clayey sediments along the northern margins of the valley as well as the wood-rich peats and fine-grained detritus-rich sediments in the south indicate deposition in a (fresh water) flood basin environment. The increase in thickness of the sedimentary unit, the amount of clay(layers) as well as the increase in fining-upward trends suggest an overall decrease in fluvio-hydraulic energy in westward direction. The combination of these features shows that Unit A3 was deposited as part of a delta system.

#### 4.5.4. Chronology

Luminescence dating of Unit A3 channel belt sands gives a 1σ age range of 78–126 ka (median age: 101 ka; Table 2), indicating a Weichselian Early Glacial (MIS 5d-a: Fig. 2) age, which is in agreement with the Unit A3 age estimate of Busschers et al. (2007) in the IJssel basin. Palynological analysis of clayey and loamy sediments in research core B14A0090 (see Table S.2 for reference) suggests that large parts of Unit A3 were deposited during the Brørup Interstadial (MIS 5c).

### 4.6. Unit A4

#### 4.6.1. Sedimentary characteristics

Unit A4 consists of coarse- to medium-grained (850-200 μm), gravelly, grey-brown coloured, calcium carbonate-rich sands. Admixed mollusc fragments, organic debris, peat fragments and clay pebbles occur concentrated at the base of the sedimentary unit (e.g. B25E0913: Fig. 4F; Fig. S.6A). Unit A4 strongly contrasts with the underlying sedimentary units because of its coarser grain-size. Cross-bedded sedimentary structures and 5–7 m thick fining-upward sequences occur regularly, especially in

the most downstream transect F (e.g. B25E0913: Fig. 4F; Fig. S.6A).

#### 4.6.2. Geometry

Unit A4 is located outside the incised valley, in the southern part of the Central Depocentre (e.g. Fig. 4A; Fig. 4D; Fig. 4F). This sedimentary unit overlies the infill of the Amsterdam and Haarlem glacial basins in the west (transect D and F: Fig. 4D; Fig. 4F). Its width varies between 14 and 25 km (Table 1). The average thickness of the sedimentary unit is 3–8 m and increases in downstream direction to ca. 11 m (Table 1). The concentration of reworked material at its base demonstrates that the lower bounding surface of Unit A4 is erosive and truncates older deposits.

#### 4.6.3. Interpretation

The brownish coloured carbonate-rich sands indicate that the sediments of Unit A4 are of Rhine origin. The cross-bedded sedimentary structures and thick fining-upward sequences, suggest that deposition occurred in deep fluvial channels, possibly of meandering style (cf. Miall, 1996; Bridge, 2003).

#### 4.6.4. Chronology

Luminescence dating of Unit A4 sediments provided a 1σ age range of 47–69 ka (median age: 57 ka; Table 2) suggesting deposition during the Weichselian Early Pleniglacial (MIS 4) and the earliest part of the Weichselian Middle Pleniglacial (MIS 3: Fig. 2). The Uranium–Thorium date of 118 ± 6 ka from a *Venerupis* sp. mollusc, formerly thought to represent the top deposits of the Eemian interglacial marine sequence in the Amsterdam-Terminal borehole (Van Leeuwen et al., 2000), is now regarded an ambivalent maximum age since the marine mollusc occurs in the fluvially reworked channel lag material of Unit A4 (B25E0913: Fig. S.6A).

### 4.7. Unit A5

#### 4.7.1. Sedimentary characteristics

Unit A5 consists of coarse- and medium-grained (800-300 μm), grey-brown coloured sands. The sands regularly contain gravel, are rich in calcium carbonate and show cross-bedded structures (e.g. B15G0212-0214: Fig. A.3; Fig. S.5C-D; Fig. S.5F). Both coarsening- and fining-upward sequences occur on a 4–6 m vertical scale, where the latter seems to dominate in this sedimentary unit. Especially in the more upstream and central transects A-C (Fig. 4A–C) the top of the sedimentary unit generally consists of medium-to fine-grained (loamy) sands (130–300 μm) with micas and detritus. The near complete absence of admixed molluscs, peat fragments and clay pebbles (only locally occurring in the basal part of Unit A5 (e.g. B16C0043: Fig. A.1; B15G0212–0213 and B20E0063: Fig. A.3) clearly distinguishes this sedimentary unit from the lower sedimentary units. The lower bounding surface of Unit A5 is erosive and dissects parts of underlying and neighbouring Units A2, A3, A4 and M1 (e.g. Figs. 4A–F; Fig. A.3; Fig. S.5D; Fig. S.5G).

#### 4.7.2. Geometry

Unit A5 occurs in large parts of the upstream and central parts of the incised Rhine-valley, here it reaches its maximum width of ca. 43 km (Fig. 4D; Table 1). This sedimentary unit also occurs in the southern part of the Central Depocentre, outside the incised valley, where it partly overlies the glacial basin fill deposits (e.g. Fig. 4F). Here, the unit's maximum thickness of 12 m is reached, presumably due to compaction of the underlying Eemian interglacial shallow-marine deposits.

#### 4.7.3. Interpretation

The brownish coloured, carbonate rich, cross-bedded deposits of Unit A5, containing both coarsening- and fining-upward sequences, are interpreted as amalgamated fluvial channel belt deposits of the Rhine. The large width of these deposits probably represents a wide braided channel–belt complex, formed by lateral channel migration and/or switching (cf. Miall, 1985). The regionally occurring fine-grained top of the sedimentary unit is interpreted as an overbank deposit (cf. Busschers et al., 2007).

#### 4.7.4. Chronology

Unit A5 is luminescence dated to a 1σ age range of 37–54 ka (median age: 43 ka; Table 2), placing deposition of this sedimentary unit in the Weichselian Middle Pleniglacial (MIS 3: Fig. 2). In addition, pollen assemblages (e.g. B15H0056–57 and B20F0175: Fig. A.2; Fig. S.4E-F-G) show high percentages of *Pinus* and grasses, indicating cold open-tundra conditions, that prevailed during the Weichselian Pleniglacial (Zagwijn, 1974; Van Huissteden et al., 2001).

### 4.8. Local fluvial and aeolian sediments

Throughout the study area fine-grained (100–150 μm), calcium carbonate-poor, well-sorted sands cover the Rhine sediments. The presence of small-scale ripples and homogeneous lithology indicates that the deposits originate from local fluvial and aeolian processes (Schokker and Koster, 2004). The thickness of this sedimentary unit increases from a few metres (2–4 m) in the southern part of the Central Depocentre, to 8–10 m in the north (Fig. 4C). Its top is often cryoturbated and/or rooted (e.g. B15F1501: Fig. A.2; Fig. S.5A, B15G0212-213-214: Fig. A.3; Fig. S.5C; S.5F). Coarser-grained sediments occasionally intercalate with the fine-grained deposits along the flanks of the ice-pushed ridges (e.g. Fig. 4A), representing local fan or slump deposits (Busschers et al., 2007).

Pollen assemblages indicate a dominance of grasses and *Pinus* (e.g. B15H0056: Fig. A.2, Fig. S.4E and B16A1292 Fig. A.1), suggesting cold, open-tundra conditions (Bunnik, 2011; Table S.2). A 1σ luminescence age range of 14–33 ka (median age: 22 ka; Table 2) was obtained for these sediments, indicating deposition during the Late Weichselian. This is comparable to earlier dating results of similar sediments in the central and southern Netherlands (Schokker et al., 2005; Busschers et al., 2007).

Holocene sediments of estuarine, lagoonal and fluvial origin cover the Late Weichselian sequence (e.g. Wiggers et al., 1962; Westerhoff et al., 1987; Cohen et al., 2009). At some locations these sediments have an erosive base which dissects the Late Weichselian deposits (e.g. Fig. 4F). The Holocene sediments are outside the scope of this paper and are therefore not further described here.

## 5. Palaeogeographical evolution and forcings

The palaeogeographical evolution of the study area is discussed below in the context of inherited glacial topography and proxy-based reconstructions of sea-level change, glacio-isostasy and climate variation. The discussion is based on six palaeogeographical maps representing key-stages in the evolution of the Rhine (Fig. 7). These maps are a compilation of new sedimentary and chronological insights obtained in this study and data from earlier work (e.g. Busschers et al., 2007, 2008; Peeters et al., 2015). Complementary to these maps, a schematic longitudinal section along the late Middle and Late Pleistocene Rhine in the central Netherlands shows the sedimentary architecture of its incised-valley fill (Fig. 8).

### 5.1. Late Saalian

During the maximum ice-cover extent of the Saalian Drenthe Substage glaciation, the Rhine and Meuse were positioned south of the Haarlem-Utrecht-Nijmegen ice-pushed ridges-line (Fig. 1B) forming part of a proglacial system that drained water and sediments from the ice-sheet in westward direction (Thomé, 1959; Van de Meene and Zagwijn, 1978; Van den Berg and Beets, 1987; Busschers et al., 2008: their Unit S4). During initial ice-sheet disintegration, both the Rhine and Meuse remained positioned in the Southern Depocentre forming a deep incised-valley system (Unit S5: Busschers et al., 2008; Hijma et al., 2012).

Continuous melting of the ice-sheet led to the exposure of a deeply scoured subglacial-basin topography and formation of lake systems in the central Netherlands (i.e. the Holland Lake: De Gans et al., 2000; Beets and Beets, 2003) and in the eastern Netherlands (i.e. the IJssel Valley lake: Busschers et al., 2008) (Fig. 7A). It was suggested by Busschers et al. (2008) that the Holland Lake system was part of a larger proglacial North Sea lake. After the Drenthe Substage deglaciation, the Rhine avulsed towards a position north of the ice-pushed ridges. It occupied the Central Depocentre, where it started to build a delta into the IJssel Valley lake (Twello Member cf. Westerhoff et al., 2003). Fine-grained Rhine sediments were also transported further westwards into the Holland Lake (Beets et al., 2006). In the Southern Depocentre the Meuse remained active as a separate system (part of Unit S5: Busschers et al., 2008; Hijma et al., 2012).

Drainage of the central Netherlands lake system resulted in deep incision, creating a 10–20 km wide valley in the Central Depocentre. The basal infill of the valley shows that during the early stage of valley formation there was still significant input of sediments from easterly sources (whitish-coloured part of Unit S6) indicating that northern drainage pathways in Germany were probably still blocked by the disintegrating ice-sheet or may have been controlled by glacio-isostatic uplift (Winsemann et al., 2015).

After completion of deltaic infilling of the IJssel basin, the Rhine secured its course into the incised valley (Fig. 7A) and started depositing coarse-grained brownish sands (Unit S6) on top of the whitish-coloured basal infill of the valley (Fig. 8). Simultaneously, the valley laterally extended towards the north (Fig. 4C–F). The coarse-grained nature of these channel belt sediments shows that deposition of these Rhine sediments occurred under periglacial conditions.

Eemian sea-level data (discussed in section 6) shows that the study area was uplifted several tens of metres, both during and directly after the Saalian glaciation. This uplift is regarded a glacio-isostatic response to loading of the lithosphere by the Fenno-scandian ice-mass in the north, which isostatically depressed the earth's crust below the ice sheet. As a counter-active response, a peripheral upwarped zone or forebulge developed at some distance around the ice-sheet (Busschers et al., 2008). The deep incision of the Rhine valley in the Central Depocentre and its typical asymmetrical shape - with its deepest part occurring in the south - may partly reflect a counter-active response to uplift and tilting effects of the study area as it was positioned on the southern flank of the forebulge crest. Initial valley formation and deepest incision in the south of the Central Depocentre is hereby envisaged during the period of maximum uplift and southward tilt followed by northward widening of the valley and aggradation during collapse of the forebulge. Similar mechanisms were proposed to have controlled late Saalian incised-valley formation in the Southern Depocentre (Busschers et al., 2008) as well as incision and valley widening patterns of the Rhine during younger periods (see section 5.4).

### 5.2. Eemian interglacial

At the onset of the Eemian interglacial in northwest Europe, temperatures rapidly increased towards values as high or higher than present (e.g. Kukla et al., 2002; Kaspar et al., 2005; Bauch and Kandiano, 2007; Brewer et al., 2008; Sturevik-Storm et al., 2014). Eustatic sea-level exceeded modern levels by at least 5.5 m (Kopp et al., 2009; Dutton and Lambeck, 2012), with average sea-level rise rates of 1.6 m per century (Rohling et al., 2008). Although reported sea-level rise-rates for the Netherlands were similar (Beets and Beets, 2003), maximum interglacial sea-level high-stand sediments are not reported above levels of −8 m below m.s.l. in The Netherlands (Zagwijn, 1983). This difference was commonly regarded to be the result of continued tectonic subsidence only, however a prolonged and delayed glacio-isostatic rebound response can now be taken into consideration too (see section 5.1 above and section 6 below).

During the early part of the Eemian (PAZ E1-E3), the Rhine remained at its position through the IJssel basin and consolidated its course through the east-west running incised valley (Fig. 7B). Early Eemian interglacial Rhine sediments (Unit A1) were deposited on top of the glacio-fluvial deposits of Unit S6 (Fig. 8). The inferred meandering fluvial-style and higher clay content in the channels reflects a more evenly-distributed discharge regime due to early Eemian interglacial climate warming, disappearance of permafrost and the development of a deciduous forest in the catchment at that time (e.g. Zagwijn, 1989, 1996). Although the periglacial supply of sediments was already terminated, there was still a lot of coarse-material present in the Rhine system due to reworking of older sediments. South of the incised Rhine-valley, lake environments fed by rainfall and groundwater seepage existed in the glacial basins of Amsterdam and Amersfoort (Fig. 7B; De Gans et al., 2000; Van Leeuwen et al., 2000).

Soil formation and the widespread occurrence of soil-protective forest vegetation during the latter part of the Eemian (PAZ E4-E5), led to a strong decrease in the amount of sediment delivered to the Rhine. In combination with the rising interglacial sea-level and increase in accommodation space, these new conditions induced a shift of the Rhine's fluvial style towards a more fine-grained anabranching-system (Fig. 7C). During this transition, fluvial wetland environments formed, marking the large-scale drowning of the incised valley due to the rising groundwater table (PAZ E3/E4a in e.g. B15F1501: Fig. A.2; B15G0212-213-214: Fig. A.3). Ongoing drowning resulted in the formation of a fluvial-tidal flood basin environment (Unit A2) (Fig. 8), which was probably semi-permanently flooded due to the nearby presence of the Rhine river mouth (B15G1501: Fig. A.2). Simultaneous to the drowning of the incised Rhine-valley during PAZ E3, rising groundwater and lake levels occurred in the former glacial basins. Already during PAZ E4a, ongoing sea-level rise led to the overtopping of the sills and inundation of the basins by the interior shelf sea, resulting in the formation of brackish-water lagoons (De Gans et al., 2000; Van Leeuwen et al., 2000).

In the incised valley, the most westward fluvial-tidal flood basin sediments of Unit A2 (Fig. 4E) were the first to experience marine inundation due to the rising interglacial sea-level (Fig. 8). This transgression transformed the fluvial-tidal flood basin into an estuary (Fig. 7C). High-stand was reached during the PAZ E4b to E5 transition (cf. Zagwijn, 1983; e.g. B15F1501: Fig. 5). The absence of well-developed tidal indicators such as mud drapes and bidirectional current ripples indicates that the estuary experienced only minor tidal influence and was probably dominated by fluvial processes. This micro-tidal regime was most likely a result of its protected inland setting within the incised-valley and the presence of

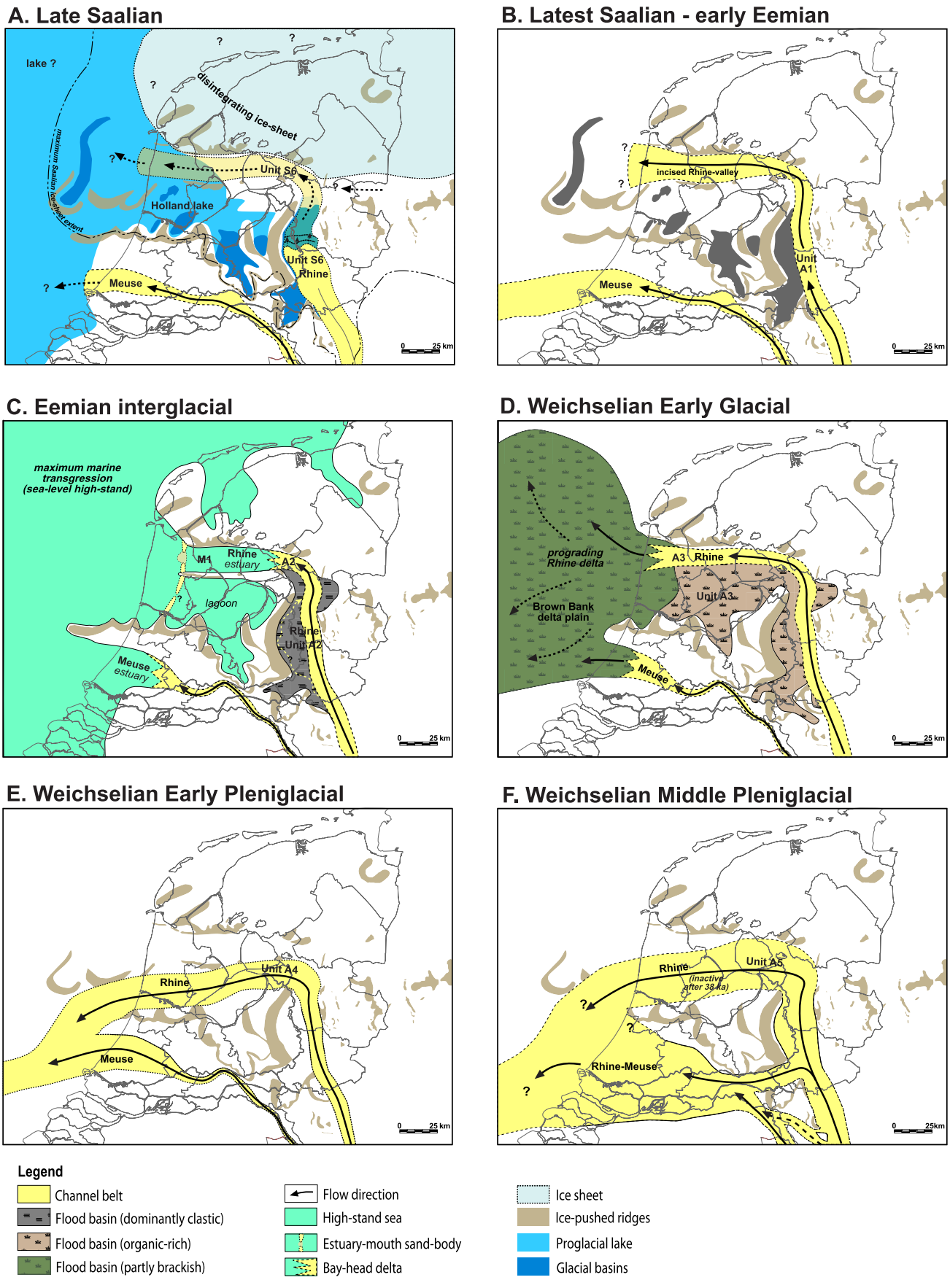
A. Late Saalian
lake ?
disintegrating ice-sheet
maximum Saalian lacustrine extent
Unit S6
Holland lake
Unit S6
Rhine
Meuse
B. Latest Saalian - early Eemian
incised Rhine-valley
Unit A1
Meuse
C. Eemian interglacial
maximum marine transgression (sea-level high-stand)
Rhine estuary
M1
A2
lagoon
Rhine Unit A2
Meuse estuary
D. Weichselian Early Glacial
prograding Rhine delta
A3 Rhine
Unit A3
Brown Bank delta plain
Meuse
E. Weichselian Early Pleniglacial
Unit A4
Rhine
Meuse
F. Weichselian Middle Pleniglacial
Rhine
Unit A5
(inactive after 38 ka)
Rhine-Meuse
0 25 km
Legend
Channel belt
Flood basin (dominantly clastic)
Flood basin (organic-rich)
Flood basin (partly brackish)
Flow direction
High-stand sea
Estuary-mouth sand-body
Bay-head delta
Ice sheet
Ice-pushed ridges
Proglacial lake
Glacial basins

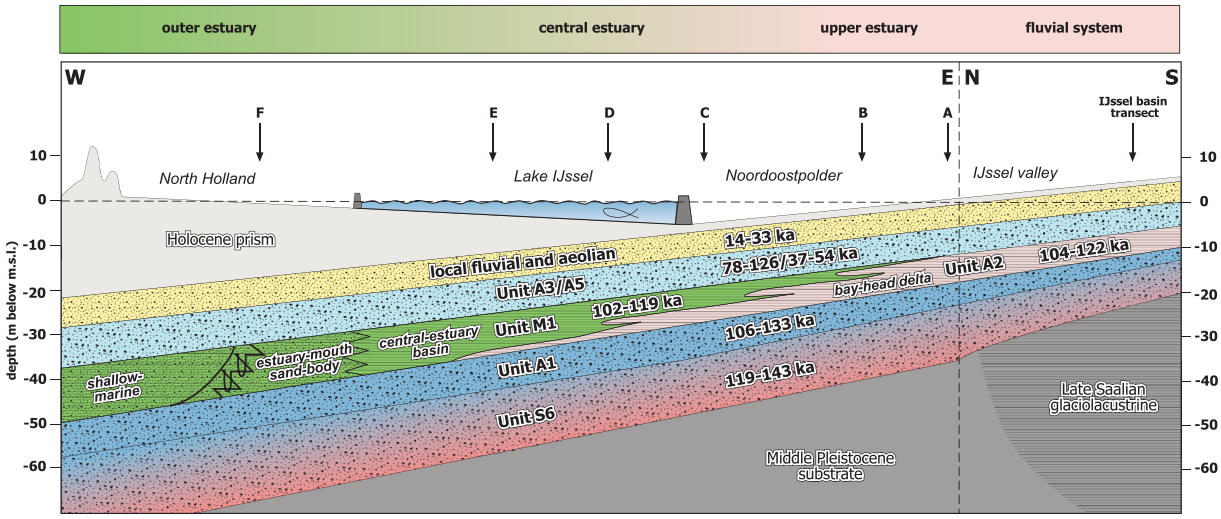


**Fig. 8.** Synthesizing schematic longitudinal section along the late Middle and Late Pleistocene Rhine in the central Netherlands (after Peeters et al., 2015), showing the sedimentary architecture of its incised-valley fill, with emphasis on the Eemian interglacial lower-deltaic setting. Luminescence ages are presented with their 1 σ uncertainty. The position of the geological transects A-F are indicated at the top of the diagram, including the position of the IJssel basin transect of Busschers et al. (2007). See main text for further descriptions and Fig. 4 for the legend.

(subaqueous) barriers (see below) and shoals at its entrance (De Gans et al., 2000).

During high-stand, a bay-head delta formed at the most upstream part of the estuary (below the present Noordoostpolder: Fig. 1; Fig. 7C; Fig. 8), where it was fed by upstream channel belts in the IJssel basin. The bay-head delta probably acted as a trap for coarser-grained sediments, resulting in only small quantities of sand reaching the central-estuary basin (below the present Lake IJssel: Fig. 1; Fig. 7C; Fig. 8). Downstream of the central basin, in the outer-estuary, an estuary-mouth sand-body developed, probably with (subaqueous) barriers onlapping onto the northern and southern margins of the incised valley (below North Holland: Fig. 1; Fig. 7C; Fig. 8). This feature probably created the protected, low energy-environment of the Eemian interglacial Rhine estuary. Given the lack of coarse-grained sediments transported to the river mouth, the estuary-mouth sand-body likely formed through reworking of local sediments by shallow-marine processes. Along the northern margin of the valley an estuary-marginal environment was present for most of the interglacial (at the location of core B15F1501 in transect C: Fig. 4C; Fig. A.2). Compared to the central axis of the estuary, the Eemian transgressive sequence is better preserved here, as is shown by its thickness of ca. 10 m (both Units A2 and M1 combined; Fig. A.2) and the near-complete Eemian pollen record.

During the same period, an uninterrupted transition from transgressive to high-stand conditions was observed in the southern part of the Central Depocentre (research cores B25E0913: Fig. S.6A; B25E0907: Fig. S.6B). Here, barriers - including beaches - developed on top of lagoonal deposits (De Gans et al., 2000; Van Leeuwen et al., 2000: Fig. 4D). Locally, in particular around the margins of the Amersfoort glacial basin, the lagoonal deposits were covered by peat-bogs. This peat formation started during PAZ E6 and continued into the Weichselian Early Glacial (Zagwijn, 1961; Cleveringa et al., 2000). During the late Eemian (PAZ E6), regression initiated a transition towards a more terrestrial, boreal environment (e.g. research core B15F1501: Fig. 5; Fig. 6).

### 5.3. Weichselian Early Glacial

Significant climatic cooling marked the onset of the Weichselian Early Glacial (Fig. 2). This period was characterised by an alternation of cold stadial conditions (Herning, Rederstall) and phases of more temperate interstadial climate (Brørup, Odderade; Caspers and Freund, 2001; Helmens, 2014). Sea-level data suggests that eustatic sea-level eventually dropped below −40 m during the stadials (Fig. 2; Waelbroeck et al., 2002) and that it reached levels of 10 m below present m.s.l. during the interstadials. Recent data however indicates that eustatic sea-level probably did not drop below −20 m for the entire period up to the Brørup Interstadial (Medina-Elizalde, 2013).

During the early phase of the Weichselian Early Glacial, the Rhine (Unit A3) retained its course in the IJssel basin (Busschers et al., 2007) and continued through the central Netherlands (Fig. 7D). Clear evidence was found for Weichselian Early Glacial Rhine channel belts at the northern part of the incised valley

**Fig. 7.** Palaeogeographic evolution of the Rhine system during the late Middle (MIS 6) and Late Pleistocene (MIS 5-3) shown in 6 successive timeframes. A) After the Drenthe Substage deglaciation, the Late Saalian Rhine-system (Unit S6) avulsed towards a position north of the ice-pushed ridges complex, progressing into the IJssel Valley and Holland lakes. Drainage of these lakes resulted in incision by the Rhine; B) After the lake drainage phase, the Latest Saalian to early Eemian Rhine (Unit A1), remained at its position through the IJssel basin and consolidated its course inside the east-west oriented incised Rhine-valley, flowing through the Central Depocentre towards the North Sea; C) Eemian interglacial sea-level high-stand. The fluvial-tidal flood basin of the Rhine (Unit A2) is located in the eastern part of the incised valley and forms the downstream continuation of the fresh-water flood basin deposits found in the IJssel basin. Marine water transgressed from the west, forming the Eemian interglacial Rhine estuary (Unit M1) with its tripartite zonation: comprising an upstream bay-head delta, a central-estuary basin and an estuary-mouth sand body with (subaqueous) barriers and tidal inlet(s) at its entrance; D) During the Weichselian Early Glacial the Rhine (Unit A3) was located in the northern part of the incised valley, while its organic-rich flood basin deposits were widely spread throughout the Central Depocentre. In the west, the prograding Rhine delta entered a partly brackish flood basin environment (i.e. Brown Bank delta plain); E) The Weichselian Early Pleniglacial Rhine (Unit A4) entered the Central Depocentre by its 'southern entry', and was for the first time positioned outside the incised Rhine-valley, in the southern part of the Central Depocentre; F) During the Weichselian Middle Pleniglacial, the Rhine (Unit A5) entered the Central Depocentre from the east by both its northern and southern entries. Around ca. 38 ka the Rhine avulsed towards the south where it merged with the Meuse, resulting in the final abandonment of the Central Depocentre by the Rhine.

(Fig. 7D). The presence of reworked marine indicators (i.e. mollusc fragments) shows that as a response to sea-level lowering at the Eemian to Weichselian Early Glacial transition, these channel belts started to incise into the Eemian interglacial estuarine deposits (Fig. 8) and reworked or eroded these (e.g. in Fig. A.2 and Fig. A.3). The channel belts were flanked by extensive flood basins consisting of alternations of wood-rich peat with humic-clay layers. Close to the ice-pushed ridges, peat growth was controlled by seepage-fed groundwater.

Throughout the Central Depocentre, relatively tranquil conditions prevailed for most of the Weichselian Early Glacial, suggesting that large-scale input of hillslope-derived sediments from the Rhine catchment was still limited due to a persisting boreal forest cover and possibly the influence of resistant (Rocourt) soil-complexes (Haesaerts and Mestdagh, 2000). This implies that the coarse-grained Weichselian Early Glacial Rhine channel belts mainly consisted of reworked older Rhine deposits, as is reflected in the large channel lag concentrate. The suggested absence of Weichselian Early Glacial channel belts in the IJssel basin (Busschers et al., 2007) is now regarded less likely since *parts* of the fluvial sediments in the IJssel basin previously interpreted as Weichselian Early Pleniglacial channel belts (Unit A4) might actually be older.

In the most western part of the Central Depocentre (i.e. Noord Holland; Fig. 1) the Weichselian Early Glacial record reached its maximum thickness of about 15 m. Similar organic-rich, fine-grained sediments that occurred in the nearby offshore region westward of North Holland (Brown Bank Formation; Laban, 1995; Westerhoff et al., 2003), show that at least part of this record was formed under brackish to marine conditions (Laban, 1995). The position of the brackish-water indicators suggest a sea-level position ca. 20 m lower than the maximum sea-level during the Eemian interglacial. This is in agreement with the estuarine sediments and shallow-marine conditions found in the Southern Depocentre for at least part of the Weichselian Early Glacial (Busschers et al., 2007: their Unit B1).

The westward increase in thickness of the Weichselian Early Glacial record and the transition into a brackish-water environment suggests that the sediments were deposited in the upstream part of a delta-system (cf. Hijma et al., 2012). A combination of luminescence and pollen data suggests that this phase of delta formation likely occurred during the Brørup Interstadial (MIS 5c: Fig. 2; Fig. 7D). The westward shift of the depocentre compared to the Eemian, is explained as an effect of upstream reduction in accommodation-space due to lower Weichselian Early Glacial relative sea-levels compared to the Eemian interglacial, as demonstrated by the thin Weichselian Early Glacial Rhine record in the IJssel basin (Busschers et al., 2007). Except for a thin record in the IJssel basin, direct evidence for Odderade-interstadial age deltaic sediments were not encountered in the study area. This is probably due to a combination of lower eustatic sea-level (MIS 5a: Fig. 2; Waelbroeck et al., 2002) as well as the fact that most onshore accommodation space was already infilled during the Brørup Interstadial. These youngest Weichselian Early Glacial deltaic sediments are expected to be present in buried position further downstream below the present North Sea.

### 5.4. Weichselian Early and Middle Pleniglacial

At the Weichselian Early Glacial to Weichselian Early Pleniglacial transition climate strongly deteriorated, resulting in a decrease in vegetation-cover and development of continuous permafrost in large parts of northwest Europe (Huijzer and Vandenberghe, 1998; Helmens, 2014). The resulting decrease in soil permeability and decrease in evapotranspiration led to larger peak-discharges of the fluvial regime in the Rhine catchment (Vandenberghe and Pissart, 1993; Busschers et al., 2007). Ice-sheet reconstructions indicate that during the Weichselian Early Pleniglacial major expansion of the Scandinavian and British ice sheets occurred (Svendsen et al., 2004; Ehlers et al., 2011; Gibbard and Clark, 2011; Houmark-Nielsen, 2011; Mangerud et al., 2011). Glacio-isostatic modelling results show that ice-sheet expansion caused significant glacio-isostatic movements and formation of a forebulge in the southern North Sea area (Lambeck et al., 2006, 2010). Ice-sheet development resulted in a significant drop of eustatic sea-level to values below −50 m (Fig. 2; Waelbroeck et al., 2002).

During the Weichselian Early Pleniglacial the Rhine entered the Central Depocentre by its 'southern entry' in the east (transect A: Fig. 4A) and was positioned south of and outside the incised valley for the first time (Unit A4; Fig. 7E). The data shows evidence for strong vertical incision (>10 m) and extensive lateral erosion at that time (Unit A4; Fig. 7E), a feature also reported for the Meuse in the Southern Depocentre (Törnqvist et al., 2000; Wallinga et al., 2004; Busschers et al., 2005, 2007). The erosion of the Rhine is attributed to a combination of strong sea-level lowering and development of large, laterally migrating (spring-snowmelt fed) channels during the early, wetter part of the Weichselian Early Pleniglacial (Guiot et al., 1989; Hatté et al., 2001).

The Rhine severely truncated Eemian, Weichselian Early Glacial and older Middle Pleistocene deposits as is clearly demonstrated by the basal concentrate of reworked material (e.g. B25E0913: Fig. S.6A). In the west, the Rhine partly truncated the Eemian shallow-marine deposits of the Haarlem and Amsterdam basins (Fig. 4F). Here, lateral erosion was particularly efficient due to the presence of easily erodible mollusc-rich sandy deposits, which also occurred in the Southern Depocentre (Busschers et al., 2007). Further upstream, lateral erosion was less pronounced due to the presence of more erosive-resistant clay and peat sequences (e.g. IJssel basin transect: Busschers et al., 2007). In the offshore region, southwest of the research area, the Rhine established a connection with the Meuse (Unit B2 of Busschers et al., 2007) in the Southern Depocentre (Fig. 7E) and jointly drained towards the Strait of Dover (Busschers et al., 2007; Hijma et al., 2012; Rijsdijk et al., 2013).

The marked southward shift of the Weichselian Early Pleniglacial Rhine outside the incised valley, and the phase of severe incision afterwards, is a pattern that resembles observations made for the Rhine-Meuse system in the Southern Depocentre during the Weichselian Late Pleniglacial (Busschers et al., 2007). Here, a similar pattern of southward migration followed by incision was related to differential, glacio-isostatic controlled tilting and upwarping of the area as a response to ice-loading in Fennoscandinavia. Since a similar forebulge feature is predicted for the Weichselian Early Pleniglacial (Lambeck et al., 2006), observations made for this period are thought to reflect the same process. The presence of a forebulge and its collapse could also explain the observations made for the Weichselian Middle Pleniglacial (see below).

During the Weichselian Middle Pleniglacial, the Rhine (Unit A5) entered the Central Depocentre from the east by both its northern and southern entries (Fig. 4A; Fig. 7F). The extensive lateral channel migration without net vertical incision (Fig. 8), together with the occupation of both entries to the Central Depocentre, suggest that minor crustal lowering occurred during the Weichselian Middle Pleniglacial. Glacio-isostatic modelling results (Lambeck et al., 2010), show a shrinking Fennoscandian ice-mass during the first part of the Weichselian Middle Pleniglacial. The reduction in forebulge height probably increased the accommodation-space, to which the Rhine responded by aggradation and northward

expansion.

Increased aggradation occurred in the IJssel basin and further upstream where it initiated a partial avulsion of the Rhine into the Southern Depocentre (Busschers et al., 2007). This avulsion led to the development of a combined Rhine-Meuse system from the early Weichselian Middle Pleniglacial onward (Unit B3 of Busschers et al., 2007) and was the first step towards complete abandonment of the Central Depocentre in a later stage. In the western part of the Central Depocentre, the Rhine bended towards the southwest (Fig. 4F; Fig. 7F), where it connected to southern drainage similar as observed during the Weichselian Early Pleniglacial.

After ca. 38 ka the Rhine abandoned its course through the Central Depocentre, hereby completing the avulsion that started in the early Weichselian Middle Pleniglacial. The Rhine and Meuse now formed a fully combined system in the Southern Depocentre (Unit B4 of Busschers et al., 2007). This major palaeogeographic rearrangement led to significant shortening of the length of the Rhine by about 65 km. Although the avulsion of the Rhine is regarded a time-diachronous process taking at least 20 kyr, overall climate cooling and increase in sediment supply and runoff reported for the period after 50 ka (including the Hasselo Stadial: Van Huissteden et al., 2001) are probably the key factors for the avulsion to complete. Probably, this process was enhanced by a rising crustal movement in the area, due to the once again growing Fennoscandian ice-cap around 39 ka (Lambeck et al., 2010).

This avulsion of the Rhine had a positive effect in terms of preservation of the older Rhine units of Eemian and Weichselian Early Glacial age: no major river activity and associated erosion occurred in the Central Depocentre during the remaining Weichselian period. The Central Depocentre's incised-valley fill was in this way protected against deep incision as was reported for the Southern Depocentre during the Weichselian Late Pleniglacial, where only very few deposits of Eemian interglacial age have been preserved (Törnqvist et al., 2000; Busschers et al., 2005).

## 6. Timing of the Eemian high-stand and implications for the Rhine deltaic system

In this study luminescence dating - both quartz OSL and feldspar pIRIR - was applied on the late Middle and Late Pleistocene sedimentary record of the Rhine (Fig. 8). The obtained luminescence-ages range from ca. 130 to 22 ka (Table 2), spanning the entire Last Interglacial–Glacial cycle. The ages of the Eemian interglacial sedimentary units, falling in the 116 to 105 ka age range, are of particular interest since they are several thousands of years younger than the widely adopted age of ca. 127-115 ka for the Eemian in northwest Europe (e.g. Kukla et al., 2002; Turner, 2002).

Methodological and/or stratigraphical issues are regarded an unlikely explanation for this striking difference. All dated sedimentary units from this study contain parts of the Eemian pollen-record (PAZ E1-E6: cf. Zagwijn, 1961, 1996) and show clear cross-cut relationships - both in sedimentary architecture and chronostratigraphy - among each other. They are constrained by younger dates from overlying sedimentary units and older luminescence-ages from lower stratigraphic levels. Furthermore, the results of both quartz OSL and feldspar pIRIR measurements are consistent *within* each sedimentary unit (Fig. 3; Table S.1), corroborating the robustness of the chronology.

Strong support for the luminescence results comes from recent paleomagnetic studies of a sequence in Germany (Neumark; Sier et al., 2011) and from research core B15F1501 presented in this study (Sier et al., 2015). By identification of the Blake Event (Smith and Foster, 1969; Channel et al., 2012) in these biostratigraphically well constrained Eemian sequences, it was shown that the Blake

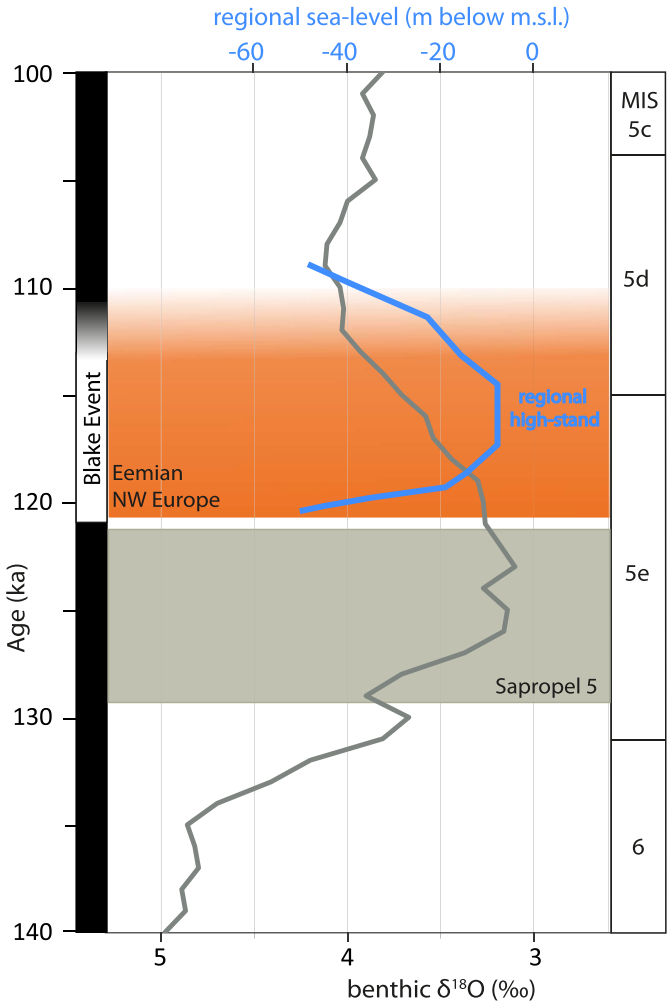


**Fig. 9.** Diagram showing the Eemian interglacial sea-level curve for the Netherlands (blue line: Zagwijn, 1983, 1996), plotted against the LR04 $\delta^{18}O$ record from 140 to 100 ka (grey line: Lisiecki and Raymo, 2005, 2009), using the Ziegler et al. (2010) time-scale. The positions of sapropel S5 (light grey area), the northwest European Eemian (orange area) and the paleomagnetic Blake Event (cf. Sier et al., 2015) are indicated.

Event in northwest Europe started just before the onset of the Eemian pollen zone E1 and lasted throughout most of the interglacial (Sier et al., 2015). By using a direct correlation to the marine isotope record (using sapropel S5: Tucholka et al., 1987; Langereis et al., 1997), where the onset of the Blake Event is placed *after* the oxygen-isotope peak-level of MIS 5e (Lisiecki and Raymo, 2009: Fig. 9), an age of ca. 121-110 ka was obtained for the Eemian interglacial in northwest Europe.

A direct consequence of a younger age for the Eemian interglacial is that the timing of the southern North Sea marine transgression also 'shifts in time' and must have lagged global eustatic sea-level by at least several thousand years (Fig. 9). It also implies that the southern North Sea sea-level high-stand took place *after* global high-stand conditions were met - i.e. during eustatic sea-level fall, and thus must reflect a *regional* sea-level high-stand (Fig. 9). This regional, late Eemian southern North Sea high-stand may be attributed to glacio-isostatic adjustment in the periphery of the former Fennoscandian ice-sheet and associated mechanisms extending to the southern North Sea near-field setting (Cohen et al., 2012; Dutton and Lambeck, 2012; Long et al., 2015), such as a prolonged and delayed rebound response to the disintegrating Saalian Fennoscandian ice-mass and to ocean-siphoning effects in

the North Atlantic ocean (e.g. Mitrovica and Milne, 2002). Presumably such processes have outweighed sea-level drawdown and need thorough further study in combination with new enhanced glacio-isostatic adjustment modelling (Van der Wal et al., 2013; De Boer et al., 2014).

The delayed timing of the high-stand in the southern North Sea had major implications for the evolution of the Rhine in the central Netherlands and adjacent southern North Sea basin. Because the southern North Sea regional high-stand took place when eustatic sea-level was already falling, regional high-stand in this area only lasted for a relatively short period of time ($\leq$3 kyr: part of PAZ E5 cf. Zagwijn, 1996, Fig. 9). As a result the total duration of sea-level driven enhanced accommodation space was also relatively short and probably not long enough to completely fill the incised valley. If the Eemian interglacial high-stand in the southern North Sea Basin would have lasted longer - for instance equal to the ca. 12 kyr as found in southwest Europe (i.e. MIS 5e plateau of Shackleton et al., 2002) - the Rhine could have probably expanded its deltaic system much further westward, hereby covering large parts of the northwestern Netherlands and adjacent North Sea. Owing to the accommodation space that remained as a consequence of the brevity of the high-stand, Rhine deltaic deposits accumulated in the Central Depocentre during the Weichselian Early Glacial (Brørup Interstadial) (Fig. 7D).

## 7. Conclusions

In this study new high-resolution core material, archived borehole-data, CPTs and 3D voxel-model results of the Eemian interglacial Rhine system were integrated. Combined with extensive luminescence dating and palaeobiological analyses, this resulted in a detailed reconstruction of the sedimentary architecture and the palaeogeographical evolution of the Rhine system during the late Middle and Late Pleistocene. Its development as an incised-valley fill in the central Netherlands holds six phases of major transition that are represented in its palaeogeographic, architectural and sedimentary expression. These transitions were caused by a combination of climate change, sea-level change and glacio-isostasy.

First, a distinct decrease in sand grain-size, an increase in clay content and a change in fluvial style from braided to meandering at the late Saalian (MIS 6) to Eemian interglacial (MIS 5e) transition is observed. This transformation is attributed to climate change and associated decrease in river peak-discharges and increased vegetation cover in the Rhine catchment.

Second, a near-total alteration of the Rhine into a fine-grained river-mode occurred in the early Eemian (MIS 5e). This change was controlled by a sea-level driven rise in base-level, transforming the study area into a fluvial-tidal flood basin. Subsequent transgression of the Eemian interglacial Rhine system, transformed the fluvial flood basin into an estuarine system. The timing of this transgression is delayed when compared to the eustatic sea-level record, suggesting that at the onset of the Eemian interglacial the area was still glacio-isostatically uplifted as a result of glaciation in the Late Saalian.

Third, relatively tranquil conditions prevailed during most of the Weichselian Early Glacial (MIS 5d-a), although erosion of the Eemian interglacial high-stand deposits occurred. In the west, continuing sedimentation by the Rhine resulted in the formation of a prograding delta. This westward shift in deposition is explained by the reduction in accommodation space caused by the base-level lowering associated with this period.

Fourth, dramatic sea-level lowering at the onset of the Weichselian Early Pleniglacial (MIS 4), combined with glacio-isostatic crustal movements, caused large-scale displacement of the Rhine system. The Rhine shifted towards a position south of the incised-valley in the Central Depocentre. Subsequently, no Weichselian Early Pleniglacial fluvial Rhine deposits form part of the incised-valley fill record.

Fifth, significant erosion occurred at the onset and during the Middle Weichselian (MIS 3). This large-scale erosion created distinct bounding surfaces which are formed by lag deposits containing reworked Eemian interglacial and Weichselian Early Glacial components. Along the margins of the incised valley this erosion was less severe, resulting in the near-complete preservation of interglacial sediments at these locations. Erosion was controlled by a combination of sea-level fall and major climatic-induced changes in sediment supply and discharge. An overall increase in the amount of sand and transition into a braided river-mode reflects the periglacial conditions that characterised the river catchment of the Rhine during the Middle Weichselian.

The final transition of the Rhine system was the avulsion in the eastern Netherlands, which led to the abandonment of the Central Depocentre by the Rhine after 38 ka. This avulsion - facilitated by climate driven aggradation and probably renewed glacio-isostatic uplift of the study area – caused a major change in drainage configuration in the central Netherlands. The avulsion had a significant effect on the preservation of the Late Pleistocene incised-valley fill. The sedimentary succession - including the Eemian interglacial estuary and fluvial-tidal flood basin sediments - did not experience significant erosion afterwards, resulting in its incorporation in the sedimentary record.

## Author contribution

JP: lead author, research design, coring, sampling and dating campaign, geological interpretation; FSB: second author, principal investigator, research design, geological interpretation; ES: principal investigator, research design; JHAB and MWvdB: geological interpretation; JW: lead scientist luminescence dating; AJV: luminescence analysis; FPMB: lead scientist pollen analysis; HM: principal investigator.

## Acknowledgements

Allard Martinius (Statoil), Sytze van Heteren (TNO-GSN) and Ad van der Spek (Deltares) are gratefully acknowledged for scientifically facilitating this research project. Heleen Koolmees and Holger Cremer (both TNO Petroleum Geosciences) are thanked for pollen and diatom analyses; Krijn Geyteman and Nico Meeuwenoord (both BAM – De Ruiter) and Ronald Folders and Jan Tuin (both Haitjema) for coring and CPTs; Wim Booltink and Henny Mensink (both TNO-GSN) for field support, core handling and description; Pieter Doornenbal and Mike van der Werf (both Deltares) for spectral gamma-ray borehole measurements and Marco de Kleine (Deltares) for various support. This research greatly benefited from discussions with Kim Cohen, Mark Sier, Janrik van den Berg (all UU), Jeroen Schokker (TNO-GSN) and Marc Hijma (Deltares). Marjan Kloos, Andre Torres and Nathan Cheshier (all former UU students) are acknowledged for their MSc-research/internship efforts. The anonymous reviewers are greatly acknowledged for improving this paper with their valuable and thoughtful comments. The Netherlands Centre for Luminescence dating (NCL) is supported by the Netherlands Organization for Scientific Research (NWO-ALW investment grant 834.03.003). This study is part of Jan Peeters' PhD-research at Utrecht University and is supported by Statoil, TNO-GSN and Deltares.

## Appendix A

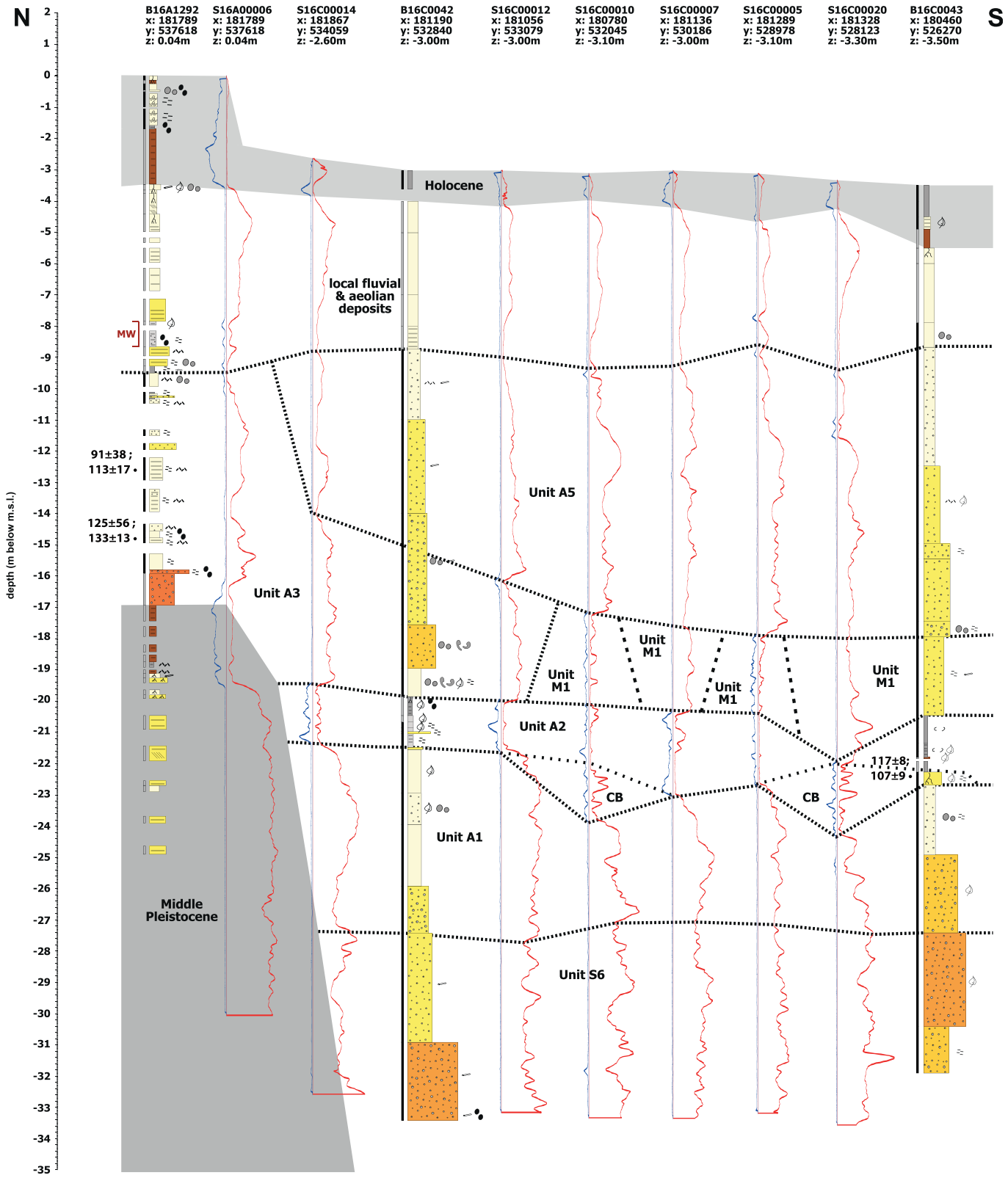


**Fig. A.1.** Sedimentary logs of transect B.

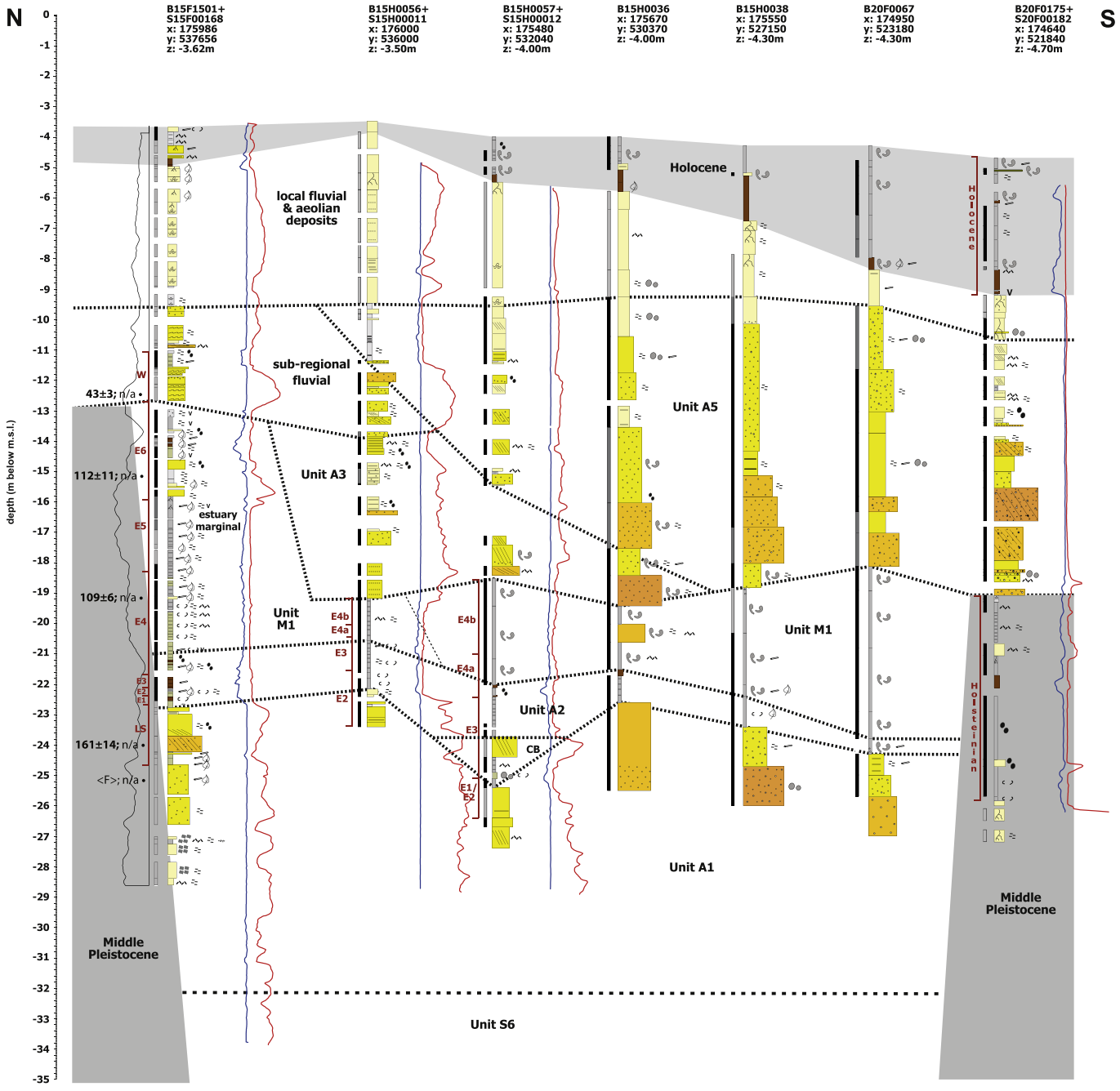


**Fig. A.2.** Sedimentary logs of transect C.

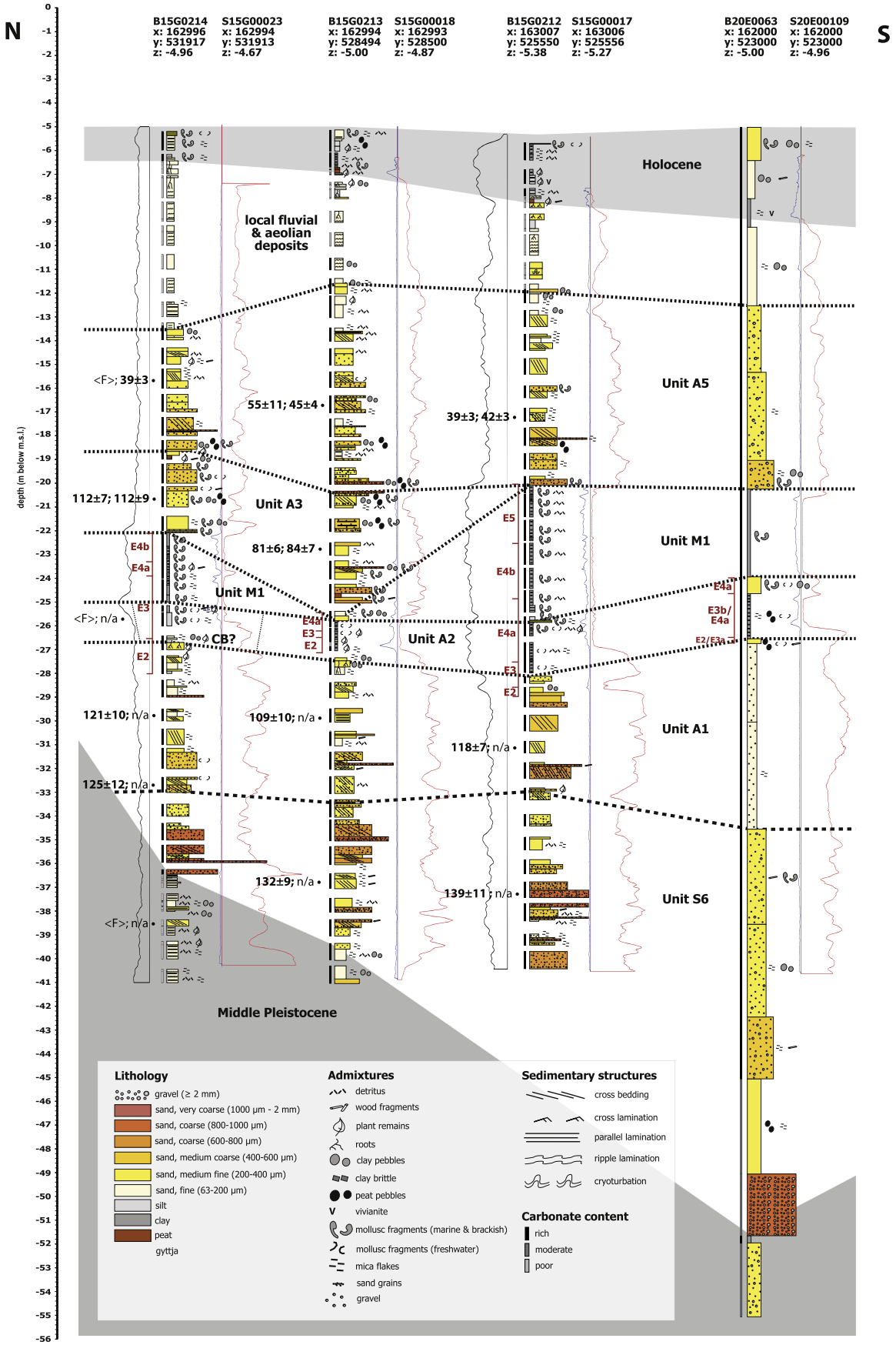


**Fig. A.3.** Sedimentary logs of transect D.

**Figure A.1–3**. Sedimentary logs, showing sedimentary unit boundaries, biostratigraphy (pollen assemblage zones cf. Zagwijn (1961, 1996)), spectral gamma-ray logs (solid black-line), cone penetration tests (solid blue- and red-lines) and luminescence ages (feldspar pIRIR: left; quartz OSL: right). Luminescence dating results with validity-label 'accepted' are presented only, solely the sample position of datings with validity-label 'rejected' are indicated: '<F>' for feldspar pIRIR and '<Q>' for quartz OSL. 'n/a' indicates the absence of the respective luminescence measurement. Core locations are plotted in Fig. 1B and are indicated on their corresponding geological transects B-D (Fig. 4B–D), the legend is shown in Fig. A.3.

## Appendix B. Supplementary data

Supplementary data related to this article can be found at http://dx.doi.org/10.1016/j.quascirev.2015.10.015.

## References


Allen, G.P., 1991. Sedimentary processes and facies in the Gironde estuary: a recent model of macrotidal estuarine systems. In: Smith, G.D., Reinson, G.E., Zaitlin, B.A., Rahmani, R.A. (Eds.), Clastic Tidal Sedimentology, Canadian Society of Petroleum Geologists Memoir 16, pp. 29–39.

Allen, G.P., Posamentier, H.W., 1993. Sequence stratigraphy and facies model of an incised valley fill: the Gironde estuary, France. J. Sediment. Petrol. 63, 378–391.

Anell, I., Thybo, H., Rasmussen, E., 2012. A synthesis of Cenozoic sedimentation in the North Sea. Basin Res. 24, 154–179.

Bassinot, F.C., Labeyrie, L.D., Vincent, E., Quidelleur, X., Shackleton, N.J., Lancelot, Y., 1994. The astronomical theory of climate and the age of the Brunhes-Matuyama magnetic reversal. Earth Planet. Sci. Lett. 126, 91–108.

Battarbee, R.W., 1973. A new method for estimation of absolute microfossil numbers, with reference especially to diatoms. Limnol. Oceanogr. 18, 647–653.

Bauch, H.A., Kandiano, E.S., 2007. Evidence for early warming and cooling in North Atlantic surface waters during the last interglacial. Paleoceanography 22, PA1201. http://dx.doi.org/10.1029/2005PA001252.

Beets, C.J., Beets, D.J., 2003. A high resolution stable isotope record of the penultimate deglaciation in lake sediments below the city of Amsterdam, The Netherlands. Quat. Sci. Rev. 22, 195–207.

Beets, D.J., Beets, C.J., Cleveringa, P., 2006. Age and climate of the late Saalian early Eemian in the type-area, Amsterdam basin, The Netherlands. Quat. Sci. Rev. 25, 876–885.

Berendsen, H.J.A., Cohen, K.M., Stouthamer, E., 2007. The use of GIS in reconstruction the Holocene palaeogeography of the Rhine-Meuse delta, The Netherlands. Int. J. Geogr. Inf. Sci. 21, 589–602.

Bierkens, M.F.P., 1996. Modeling hydraulic conductivity of a complex confining layer at various spatial scales. Water Resour. Res. 32, 2369–2382.

Blum, M.D., 1993. Genesis and architecture of incised valley fill sequences: a Late Quaternary example from the Colorado River, Gulf Coastal Plain of Texas. In: Weimer, P., Posamentier, H.W. (Eds.), Siliclastic Sequence Stratigraphy: Recent Developments and Applications, Memoir – American Association of Petroleum Geologists 58, pp. 259–283.

Blum, M.D., Törnqvist, T., 2000. Fluvial responses to climate and sea-level change: a review and look forward. Sedimentology 47, 2–48.

Blum, M.D., Martin, J., Milliken, K., Garvin, M., 2013. Paleovalley systems: Insights from Quaternary analogs and experiments. Earth Sci. Rev. 116, 128–169.

Bosch, J.H.A., 2000. Standaard Boor Beschrijvingsmethode Versie 5.1. Report NITG 00-141-A. Netherlands Institute of Applied Geosciences TNO, Utrecht, The Netherlands.

Brewer, S., Guiot, J., Sánchez-Goñi, M.F., Klotz, S., 2008. The climate in Europe during the Eemian: a multi-method approach using pollen data. Quat. Sci. Rev. 27, 2303–2315.

Bridge, J., 2003. Rivers and Floodplains – Forms, Processes and Sedimentary Record. Blackwell Science Ltd, Oxford.

Bunnik, F.P.M., 2011. Pollenanalyses van de Formatie van Boxtel uit de boring Bantega (B16A1292). Report TNO-060-UT-2011-00698/B. TNO Earth, Environmental and Life Sciences, Utrecht.

Busschers, F.S., Weerts, H.J.T., Wallinga, J., Cleveringa, P., Kasse, C., De Wolf, H., Cohen, K.M., 2005. Sedimentary architecture and optical dating of Middle and Late Pleistocene Rhine-Meuse deposits – fluvial response to climate change, sea-level fluctuation and glaciation. Neth. J. Geosci. 84, 25–41.

Busschers, F.S., Kasse, C., Van Balen, R.T., Vandenberghe, J., Cohen, K.M., Weerts, H.J.T., Wallinga, J., Johns, C., Cleveringa, P., Bunnik, F.P.M., 2007. Late Pleistocene evolution of the Rhine-Meuse system in the southern North Sea basin: imprints of climate change, sea-level oscillation and glacio-isostasy. Quat. Sci. Rev. 26, 3216–3248.

Busschers, F.S., Van Balen, R.T., Cohen, K.M., Kasse, C., Weerts, H.J.T., Wallinga, J., Bunnik, F.P.M., 2008. Response of the Rhine-Meuse fluvial system to Saalian ice-sheet dynamics. Boreas 37, 377–398.

Buylaert, J.-P., Jain, M., Murray, A.S., Thomsen, K.J., Thiel, C., Sohbati, R., 2012. A robust feldspar luminescence dating method for Middle and Late Pleistocene sediments. Boreas 41, 435–451.

Caspers, G., Freund, H., 2001. Vegetation and climate in the Early- and Pleni-Weichselian in northern central Europe. J. Quat. Sci. 16, 31–48.

Caston, V.N.D., 1979. A new isopachyte map of the Quaternary of the North Sea. In: Oele, E., Schüttenhelm, R.T.E., Wiggers, A.J. (Eds.), The Quaternary History of the North Sea, Acta Universitatis Upsaliensis, Symposium Universitatis Upsaliensis Annum Quingentesimum Celebrantis: 2, Uppsala, pp. 23–28.

Channell, J.E.T., Hodell, D.A., Curtis, J.H., 2012. ODP Site 1063 (Bermuda Rise) revisited: oxygen isotopes, excursions and paleointensity in the Brunhes Chron. Geochem. Geophys. Geosyst. 13, Q02001.

Cleveringa, P., Meijer, T., Van Leeuwen, R.J.W., De Wolf, H., Pouwer, R., Lissenberg, T., Burger, A.W., 2000. The Eemian stratotype locality at Amersfoort in the central Netherlands: a re-evaluation of old and new data. Neth. J. Geosci. 79, 197–216.

Coerts, A., 1996. Analysis of Static Cone Penetration Test Data for Subsurface Modelling – a Methodology (PhD thesis). Utrecht University, Netherlands Geographical Studies 210, The Netherlands.

Cohen, K.M., Stouthamer, E., Hoek, W.Z., Berendsen, H.J.A., Kempen, H.F.J., 2009. Zand in banen – Zanddieptekaarten van het Rivierengebied en het IJsseldal in de provincies Gelderland en Overijssel. Derde geheel herziene druk, Provincie Gelderland, Arnhem, The Netherlands.

Cohen, K.M., MacDonald, K., Joordens, J.C.A., Roebroeks, W., Gibbard, P.L., 2012. The earliest occupation of north-west Europe: a coastal perspective. Quaternary International 271, 70–83.

Cohen, K.M., Gibbard, P.L., Weerts, H.J.T., 2014. North Sea palaeogeographical reconstructions for the last 1 Ma. Neth. J. Geosci. 93, 7–29.

Cremer, H., Wagner, B., Melles, M., Hubberten, H.-W., 2001. The postglacial environmental development of Raffles Sø, East Greenland: inferences from a 10,000 year diatom record. J. Paleolimnol. 26, 67–87.

Dalrymple, R.W., Zaitlin, B.A., Boyd, R., 1992. Estuarine facies models: conceptual basis and stratigraphic implications. J. Sediment. Petrol. 62, 1130–1146.

Dalrymple, R.W., Choi, K., 2007. Morphologic facies trends through the fluvial-marine transition in tide-dominated depositional systems: a schematic framework for environmental and sequence-stratigraphic interpretation. Earth Sci. Rev. 81, 135–174.

De Boer, B., Stocchi, P., Van de Wal, R.S.W., 2014. A fully coupled 3D ice-sheet-sea-level model: algorithm and applications. Geosci. Model Dev. 7, 2141–2156.

De Gans, W., De Groot, T., Zwaan, H., 1987. The Amsterdam basin, a case study of a glacial basin in The Netherlands. In: Van der Meer, J.J.M. (Ed.), Tills and Glaciotectonics. Balkema, Rotterdam, pp. 205–216.

De Gans, W., Beets, D.J., Centineo, M.C., 2000. Late Saalian and Eemian deposits in the Amsterdam glacial basin. Neth. J. Geosci. 79, 147–160.

Dutton, A., Lambeck, K., 2012. Ice volume and sea level during the Last Interglacial. Science 337, 216–219.

Ehlers, J., Grube, A., Stephan, H.-J., Wansa, S., 2011. Pleistocene glaciations of North Germany – new results. In: Ehlers, J., Gibbard, P.L., Hughes, P.D. (Eds.), Quaternary Glaciations – Extent and Chronology, Developments in Quaternary Science, vol. 15, pp. 149–162.

Faegri, K., Iversen, J., 1989. Textbook of Pollen Analysis. In: Faegri, K., Kaland, P.E., Krzywinski, K. (Eds.), fourth ed. Wiley, Chichester.

Florschütz, F., 1935. Over Azolla en de ouderdomsbepaling van interglaciale zoetwater afzettingen in Nederland. Geol. Mijnb. 14, 12–13.

Gibbard, P.L., Clark, C.D., 2011. Pleistocene glaciation limits in Great Britain. In: Ehlers, J., Gibbard, P.L., Hughes, P.D. (Eds.), Quaternary Glaciations – Extent and Chronology, Developments in Quaternary Science, vol. 15, pp. 75–93.

Gunnink, J.L., Maljers, D., Van Gessel, S.F., Menkovic, A., Hummelman, H.J., 2013. A 3D raster model of the subsurface of the Netherlands: the Digital Geological Model (DGM). Neth. J. Geosci. 92, 33–46.

Guiot, J., Pons, A., de Beaulieu, J.L., Reille, M., 1989. A 140,000-year continental climate reconstruction from two European pollen records. Nature 338, 309–313.

Haesaerts, P., Mestdagh, H., 2000. Pedosedimentary evolution of the last interglacial and early glacial sequence in the European loess belt from Belgium to central Russia. Neth. J. Geosci. 79, 313–324.

Hatté, C., Antoine, P., Fontugne, M., Rousseau, D.D., Tisnérat-Laborde, N., Zöller, L., 2001. New chronology and organic matter $\delta^{13}C$ paleoclimatic significance of Nußloch loess sequence (Rhine Valley, Germany). Quat. Int. 62, 85–91.

Helmens, K.F., 2014. The Last Interglacial-Glacial cycle (MIS 5-2) re-examined based on long proxy records form central and northern Europe. Quat. Sci. Rev. 86, 115–143.

Hijma, M.P., Cohen, K.M., Hoffman, G., Van der Spek, A.J.F., Stouthamer, E., 2009. From river valley to estuary: the evolution of the Rhine mouth in the early to middle Holocene (western Netherlands, Rhine-Meuse delta). Neth. J. Geosci. 88, 13–53.

Hijma, M.P., Cohen, K.M., Roebroeks, W., Westerhoff, W.E., Busschers, F.S., 2012. Pleistocene Rhine-Thames landscapes: geological background for hominin occupation of the southern North Sea region. J. Quat. Sci. 27, 17–29.

Houmark-Nielsen, M., 2011. Pleistocene glaciations in Denmark: a closer look at chronology, ice dynamics and landforms. In: Ehlers, J., Gibbard, P.L., Hughes, P.D. (Eds.), Quaternary Glaciations – Extent and Chronology, Developments in Quaternary Science, vol. 15, pp. 47–58.

Huijzer, G.P., 1992. Quantitative Penetrostratigraphic Classification (PhD thesis). VU University Amsterdam, The Netherlands.

Huijzer, B., Vandenberghe, J., 1998. Climate reconstruction of the Weichselian

Pleniglacial in northwestern and central Europe. J. Quat. Sci. 13, 391–417.
Kars, R.H., Wallinga, J., Cohen, K.M., 2008. A new approach towards anomalous fading correction for feldspar IRSL dating – tests on samples in field saturation. Radiat. Meas. 43, 786–790.
Kars, R.H., Busschers, F.S., Wallinga, J., 2012. Validating post IR-IRSL dating on K-feldspars through comparison with quartz OSL ages. Quat. Geochronol. 12, 74–86.
Kars, R.H., Reimann, T., Ankjærgaard, C., Wallinga, J., 2014. Bleaching of the Post-IR IRSL Signal: New Insights for Feldspar Luminescence Dating. Boreas 43, 780–791. http://dx.doi.org/10.1111/bor.12082.
Kaspar, F., Kühl, N., Cubasch, U., Litt, T., 2005. A model-data comparison of European temperatures in the Eemian interglacial. Geophys. Res. Lett. 32, L11703.
Kooi, H., Johnston, P., Lambeck, K., Smither, C., Molendijk, R., 1998. Geological causes of recent (~100 yr) vertical land movement in The Netherlands. Tectonophysics 299, 279–316.
Kopp, R.E., Simons, F.J., Mitrovica, J.X., Maloof, A.C., Oppenheimer, M., 2009. Probabilistic assessment of sea level during the last interglacial stage. Nature 462, 863–868.
Kukla, G.J., Bender, M.L., de Beaulieu, J.-L., Bond, G., Broecker, W.S., Cleveringa, P., Gavin, J.E., Herbert, T.D., Imbrie, J., Jouzel, J., Keigwin, L.D., Knudsen, K.-L., McManus, J.F., Merkt, J., Muhs, D.R., Müller, H., Poore, R.Z., Porter, S.C., Seret, G., Shackleton, N.J., Turner, C., Tzedakis, P.C., Winograd, I.J., 2002. Last interglacial climates. Quat. Res. 58, 2–13.
Laban, C., 1995. The Pleistocene Glaciations in the Dutch Sector of the North Sea. A Synthesis of Sedimentary and Seismic Data (PhD thesis). University of Amsterdam, Amsterdam, The Netherlands.
Lambeck, K., Purcell, A., Funder, S., Kjær, K.H., Larsen, E., Möller, P., 2006. Constraints on the Late Saalian to early Middle Weichselian ice sheet of Eurasia from field data and rebound modelling. Boreas 35, 539–575.
Lambeck, K., Purcell, A., Zhao, J., Svensson, N.-O., 2010. The Scandinavian ice sheet: from MIS 4 to the end of the last glacial maximum. Boreas 39, 410–435.
Lamothe, M., Auclair, M., Hamzoui, C., Hout, S., 2003. Towards a prediction of long-term anomalous fading of feldspar IRSL. Radiat. Meas. 37, 493–498.
Langereis, C.G., Dekkers, M.J., Lange, G.J., Paterne, M., Santvoort, P.J.M., 1997. Magnetostratigraphy and astronomical calibration of the last 1.1 Myr from an eastern Mediterranean piston core and dating of short events in the Brunhes. Geophys. J. Int. 129, 75–94.
Lisiecki, L.E., Raymo, M.E., 2005. A Pliocene-Pleistocene stack of 57 globally distributed benthic d18O records. Paleoceanography 20, PA1003. http://dx.doi.org/10.1029/2004PA001071.
Lisiecki, L.E., Raymo, M.E., 2009. Diachronous benthic $d^{18}O$ responses during late Pleistocene terminations. Paleoceanography 24, PA3210. http://dx.doi.org/10.1029/2009PA001732.
Long, A.J., Barlow, N.L.M., Busschers, F.S., Cohen, K.M., Gehrels, W.R., Wake, L.M., 2015. Near-field sea-level variability in northwest Europe and ice sheet stability during the last interglacial. Quaternary Science Reviews 126, 26–40.
Martinius, A.W., Ringrose, P.S., Brostrøm, C., Elfenbein, C., Næss, A., Ringås, J.E., 2005. Reservoir challenges of heterolithic tidal sandstone reservoirs in the Halten Terrace, mid-Norway. Pet. Geosci. 11, 3–16.
Mangerud, J., Gyllencreutz, R., Lohne, Ø., Svendsen, J.I., 2011. Glacial history of Norway. In: Ehlers, J., Gibbard, P.L., Hughes, P.D. (Eds.), Quaternary Glaciations – Extent and Chronology, Developments in Quaternary Science, vol. 15, pp. 279–298.
Medina-Elizalde, M., 2013. A global compilation of coral sea-level benchmarks: implications and new challenges. Earth Planet. Sci. Lett. 362, 310–318.
Miall, A.D., 1985. Architectural-element analysis: a new method of facies analysis applied to fluvial deposits. Earth Sci. Rev. 22, 261–308.
Miall, A.D., 1996. The Geology of Fluvial Deposits. Springer, Berlin.
Mitrovica, J.X., Milne, G.A., 2002. On the origin of late Holocene sea-level highstands within equatorial ocean basins. Quat. Sci. Rev. 21, 2179–2190.
Murray, A.S., Olley, J.M., 2002. Precision and accuracy in the optically stimulated luminescence dating of sedimentary quartz: a status review. Geochronometria 21, 1–16.
Murray, A.S., Wintle, A.G., Wallinga, J., 2002. Dose estimation using quartz OSL in the non-linear region of the growth curve. Radiat. Prot. Dosim. 101, 371–374.
Murray, A.S., Svendsen, J.I., Mangerud, J., Astakhov, V.I., 2007. Testing the accuracy of quartz OSL dating using a known-age Eemian site on the river Sula, northern Russia. Quat. Geochronol. 2, 102–109.
Murray, A.S., Thomsen, K.J., Masuda, M., Buylaert, J.P., Jain, M., 2012. Identifying well-bleached quartz using the different bleaching rates of quartz and feldspar luminescence signals. Radiat. Meas. 47, 688–695.
Nanson, G.C., Knighton, A.D., 1996. Anabranching rivers: their cause, character and classification. Earth Surf. Process. Landforms 21, 217–239.
North Greenland Eemian Ice Drilling (NEEM) Community Members, 2013. Eemian interglacial reconstructed from a Greenland folded ice core. Nature 493, 489–494.
North Greenland Ice Core Project (NGRIP) Members, 2004. High-resolution record of Northern Hemisphere climate extending into the last interglacial period. Nature 431 (7005), 147–151.
Peeters, J., Busschers, F.S., Stouthamer, E., 2015. Fluvial evolution of the Rhine during the last interglacial-glacial cycle in the southern North Sea basin: a review and look forward. Quat. Int. 357, 176–188.
Rijks Geologische Dienst (RGD), 1977. Geologisch onderzoek in de bouwput te Den Helder. Intern verslag 1. Alkmaar.
Rijsdijk, K.F., Kroon, I.C., Meijer, T., Passchier, S., Van Dijk, T.A.G.P., Bunnik, F.P.M., Janse, A.C., 2013. Reconstructing Quaternary Rhine-Meuse dynamics in the southern North Sea: architecture, seismolithofacies associations and malacological biozonation. J. Quat. Sci. 28, 433–536.
Rittenour, T.M., 2008. Luminescence dating of fluvial deposits: applications to geomorphic, palaeoseismic and archaeological research. Boreas 37, 613–635.
Rohling, E.J., Grant, K., Hemleben, C.H., Siddal, M., Hoogakker, B.A.A., Bolshaw, M., Kucera, M., 2008. High rates of sea-level rise during the Last Interglacial period. Nat. Geosci. 1, 38–42.
Sanchez-Vila, X., Guadagnini, A., Carrera, J., 2006. Representative hydraulic conductivities in saturated groundwater flow. Rev. Geophys. 44, RG3002.
Schokker, J., Koster, E.A., 2004. Sedimentology and facies distribution of Pleistocene cold-climate aeolian and fluvial deposits in the Roer Valley Graben (Southeastern Netherlands). Permafr. Periglac. Process. 15, 1–20.
Schokker, J., Cleveringa, P., Murray, A.S., Wallinga, J., Westerhoff, W.E., 2005. An OSL dated Middle and Late Quaternary sedimentary record in the Roer Valley Graben (southeastern Netherlands). Quat. Sci. Rev. 24, 2243–2264.
Shackleton, N.J., Chapman, M., Sánchez-Goñi, M.F., Pailler, D., Lancelot, Y., 2002. The classic marine isotope substage 5e. Quat. Res. 58, 14–16. http://dx.doi.org/10.1006/qres.2001.2312.
Sier, M.F., Roebroeks, W., Bakels, C.C., Dekkers, M.J., Brühl, E., De Loecker, D., Gaudzinski-Windheuser, S., Hesse, N., Jagich, A., Kindler, L., Kuijper, W.J., Laurat, T., Mücher, H.J., Penkman, K.E.H., Richter, D., Van Hinsbergen, D.J.J., 2011. Direct terrestrial-marine correlation demonstrates surprisingly late onset of the Last Interglacial in central Europe. Quat. Res. 75, 213–218.
Sier, M.J., Peeters, J., Dekkers, M.J., Parés, J.M., Chang, L., Busschers, F.S.B., Cohen, K.M., Wallinga, J., Bunnik, F.P., Roebroeks, W., 2015. The Blake Event recorded near the Eemian Type locality – a diachronic onset of the Eemian in Europe. Quat. Geochronol. 28, 12–28.
Smith, J.D., Foster, J.H., 1969. Geomagnetic reversal in Brunhes normal polarity epoch. Science 163, 565–567.
Stafleu, J., Maljers, D., Gunnink, J.L., Menkovic, A., Busschers, F.S., 2011. 3D modelling of the shallow subsurface of Zeeland, the Netherlands. Neth. J. Geosci. 90, 293–310.
Sturevik-Storm, A., Aldahan, A., Possnert, G., Berggren, A.-M., Muscheler, R., Dahl-Jensen, D., Vinther, B.M., Usoskin, I., 2014. $^{10}Be$ climate fingerprints during the Eemian in the NEEM ice core, Greenland. Sci. Rep. 4, 6408.
Svendsen, J.I., Alexanderson, H., Astakhov, V.I., Demidov, I., Dowdeswell, J.A., Funder, S., Gataullin, V., Henriksen, M., Hjort, C., Houmark-Hielsen, M., Hubberten, H.W., Ingólfsson, Ó., Jakobsson, M., Kjær, K.H., Larsen, E., Lokrantz, H., Lunkka, J.P., Lyså, A., Mangerud, J., Matiouchkov, A., Murray, A., Möller, P., Niessen, F., Nikolskaya, O., Polyak, L., Saarnisto, M., Siegert, C., Siegert, M.J., Spielhagen, R.F., Stein, R., 2004. Late Quaternary ice sheet history of northern Eurasia. Quat. Sci. Rev. 23, 1229–1271.
Thiel, C., Buylaert, J.-P., Murray, A.S., Terhorst, B., Hofer, I., Tsukamoto, S., Frechen, M., 2011. Luminescence dating of the Stratzing loess profile (Austria) – testing the potential of an elevated temperature post-IR IRSL protocol. Quat. Int. 234, 23–31.
Thomé, K.N., 1959. Das Inlandeis am Niederrhein. Fortschritte der Geol. von Rheinl. und Westfalen 4, 197–246.
Thomsen, K.J., Murray, A.S., Jain, M., Bøtter-Jensen, L., 2008. Laboratory fading rates of various luminescence signals from feldspar-rich sediment extracts. Radiat. Meas. 43, 1474–1486.
Thrana, C., Næss, A., Leary, S., Gowland, S., Brekken, M., Taylor, A., 2014. Updated depositional and stratigraphic model of the Lower Jurassic Åre Formation, Heidrun Field, Norway. In: Martinius, A.W., Ravnås, R., Howell, J.A., Steel, R.J., Wonham, J.P. (Eds.), From Depositional Systems to Sedimentary Successions on the Norwegian Continental Margin. International Association of Sedimentologists, Special Publication 46, pp. 253–290.
TNO-GSN, 2014. Geological Survey of the Netherlands. TNO-GSN Subsurface Database at DINOLoket (Internet Portal for Geo-information on Netherlands' Subsurface). Data retrieved on [31-01-2014] from: http://www.dinoloket.nl.
Törnqvist, T.E., Wallinga, J., Murray, A.S., De Wolf, H., Cleveringa, P., De Gans, W., 2000. Response of the Rhine-Meuse system (west-central Netherlands) to the last Quaternary glacio-eustatic cycles: a first assessment. Glob. Planet. Change 27, 89–111.
Törnqvist, T.E., Wallinga, J., Busschers, F.S., 2003. Timing of the last sequence boundary in a fluvial setting near the highstand shoreline – insights from optical dating. Geology 31, 279–282.
Tucholka, P., Fontugne, M., Guichard, F., Paterne, M., 1987. The Blake magnetic polarity episode in cores from the Mediterranean Sea. Earth Planet. Sci. Lett. 86, 320–326.
Turner, C., 2002. Problems of the duration of the Eemian Interglacial in Europe north of the Alps. Quat. Res. 58, 45–48.
Van Balen, R.T., Houtgast, R.F., Cloetingh, S.A.P.L., 2005. Neotectonics of The Netherlands: a review. Quat. Sci. Rev. 24, 439–454.
Van de Meene, E.A., Zagwijn, W.H., 1978. Die Rheinläufe im deutsch-niederländische Grenzgebiet seit der Saale-Kaltzeit. Überblick neuer geologische rund pollenanalytischer Untersuchungen. Fortschritte der Geol. von Rheinl. und Westfalen Band 28, 345–359.
Van den Berg, M.W., Beets, D.J., 1987. Saalian glacial deposits and morphology in The Netherlands. In: Van der Meer, J.J.M. (Ed.), Tills and Glaciotectonics. Balkema, Rotterdam, pp. 235–251.
Vandenberghe, J., Pissart, A., 1993. Permafrost changes in Europe during the Last Glacial. Permafr. Periglac. Process. 4, 121–135.
Van der Meulen, M.J., Van Gessel, S.F., Veldkamp, J.G., 2005. Aggregate resources in

the Netherlands. Neth. J. Geosci. 84, 379–387.
Van der Meulen, M.J., Doornendal, J.C., Gunnink, J.L., Stafleu, J., Schokker, J., Vernes, R.W., Van Geer, F.C., Van Gessel, S.F., Van Heteren, S., Van Leeuwen, R.J.W., Bakker, M.A.J., Bogaard, P.J.F., Busschers, F.S., Griffioen, J., Gruijters, S.H.L.L., Kiden, P., Schroot, B.M., Simmelink, H.J., Van Berkel, W.O., Van der Krogt, R.A.A., Westerhoff, W.E., Van Daalen, T.M., 2013. 3D geology in a 2D country: perspectives for geological surveying in the Netherlands. Neth. J. Geosci. 92, 217–241.
Van der Wal, W., Barnhoorn, A., Stocchi, P., Gradmann, S., Wu, P., Drury, M., Vermeersen, B., 2013. Glacial isostatic adjustment model with composite 3-D earth rheology for Fennoscandia. Geophys. J. Int. 194, 61–77.
Van Huissteden, J., Kasse, C., 2001. Detection of rapid climate change in Last Glacial fluvial successions in The Netherlands. Glob. Planet. Change 28, 319–339.
Van Huissteden, J., Gibbard, P., Briant, R.M., 2001. Periglacial fluvial systems in northwest Europe during marine isotope stages 4 and 3. Quat. Int. 79, 75–88.
Van Leeuwen, R.J.W., Beets, D.J., Bosch, J.H.A., Burger, A.W., Cleveringa, P., Van Harten, D., Waldemar Herngreen, G.F., Kruk, R.W., Langereis, C.G., Meyer, T., Pouwer, R., De Wolf, H., 2000. Stratigraphy and integrated facies analysis of the Saalian and Eemian deposits in the Amsterdam-Terminal borehole, the Netherlands. Neth. J. Geosci. 79, 161–196.
Waelbroeck, C., Labeyrie, L., Michel, E., Duplessy, J.C., McManus, J.F., Lambeck, K., Balbon, E., Labracherie, M., 2002. Sea-level and deep water temperature changes derived from benthic foraminifera isotopic records. Quat. Sci. Rev. 21, 295–305.
Wallinga, J., 2002. Optically stimulated luminescence dating of fluvial deposits: a review. Boreas 31, 303–322.
Wallinga, J., Törnqvist, T.E., Busschers, F.S.B., Weerts, H.J.T., 2004. Allogenic forcing of the Late Quaternary Rhine-Meuse fluvial record: the interplay of sea-level change, climate change and crustal movements. Basin Res. 16, 535–547.
Wallinga, J., Bos, A.J.J., Dorenbos, P., Murray, A.S., Schokker, J., 2007. A test case for anomalous fading correction in IRSL dating. Quat. Geochronol. 2, 216–221.
Westerhoff, W.E., De Mulder, E.F.J., De Gans, W., 1987. Toelichtingen bij de geologische kaart van Nederland 1:50.000. Blad Alkmaar Oost en West (19O en 19W). Rijks Geologische Dienst, Haarlem, The Netherlands.
Westerhoff, W.E., Wong, T.E., Geluk, M.C., 2003. De opbouw van de ondergrond. In: De Mulder, E.F.J., Geluk, M.C., Ritsema, I., Westerhoff, W.E., Wong, T.E. (Eds.), De ondergrond van Nederland. Nederlands Instituut voor Toegepaste Geowetenschappen TNO, Utrecht, pp. 247–352.
Westerhoff, W.E., Kemna, H.A., Boenigk, W., 2008. The confluence area of Rhine, Meuse, and Belgian rivers: late Pliocene and Early Pleistocene fluvial history of the northern Lower Rhine Embayment. Neth. J. Geosci. 87, 107–125.
Wiggers, A.J., 1955. De wording van het noordoostpoldergebied – een onderzoek naar de physisch-geografische ontwikkeling van een sedimentair gebied. Van zee tot land 14, Zwolle, The Netherlands.
Wiggers, A.J., De Jong, F.H., Spanger, K., 1962. De bodemgesteldheid van de Noordoostpolder. Van zee tot land 33, Zwolle, The Netherlands.
Winsemann, J., Lang, J., Roskosch, J., Polom, U., Böhner, U., Brandes, C., Glotzbach, C., Frechen, M., 2015. Terrace styles and timing of terrace formation in the Weser and Leine valleys, northern Germany: Response of a fluvial system to climate change and glaciation. Quaternary Science Reviews 123, 31–57.
Wintle, A.G., 2008. Fifty years of luminescence dating. Archaeometry 50, 276–312.
Wintle, A.G., Murray, A.S., 2006. A review of quartz optically stimulated luminescence characteristics and their relevance in single-aliquot regeneration protocols. Radiat. Meas. 41, 369–391.
Zagwijn, W.H., 1961. Vegetation, climate and radiocarbon datings in the Late Pleistocene of The Netherlands, Part I: Eemian and Early Weichselian. Meded. Geol. Sticht. N. S. 14, 15–45.
Zagwijn, W.H., 1973. Pollen analytic studies of Holsteinian and Saalian Beds in the northern Netherlands. Meded. Rijks Geol. Dienst N. S. 24, 139–156.
Zagwijn, W.H., 1974. The palaeogeographic evolution of The Netherlands during the Quaternary. Geol. en Mijnbouw/Netherlands J. Geosci. 53, 369–385.
Zagwijn, W.H., 1983. Sea-level changes in The Netherlands during the Eemian. Geol. en Mijnbouw/Netherlands J. Geosci. 62, 437–450.
Zagwijn, W.H., 1989. The Netherlands during the tertiary and the quaternary: a case history of coastal lowland evolution. Geol. en Mijnbouw/Netherlands J. Geosciences 68, 107–120.
Zagwijn, W.H., 1996. An analysis of Eemian climate in Western and Central Europe. Quat. Sci. Rev. 15, 451–469.
Zaitlin, B.A., Dalrymple, R.W., Boyd, R., 1994. The stratigraphic organization of incised-valley systems associated with relative sea-level change. SEPM Spec. Publ. 51, 45–60.
Ziegler, P.A., 1994. Cenozoic rift system of western and central Europe: an overview. Geol. en Mijnbouw/Netherlands J. Geosciences 73, 99–127.
Ziegler, M., Tuenter, E., Lourens, L.J., 2010. The precession phase of the boreal summer monsoon as viewed from the eastern Mediterranean (ODP Site 968). Quat. Sci. Rev. 29, 1481–1490.